

1-1-2008

## Update to ANSI/ANS-643-1991 for high-Z materials and review of particle transport theory

Lawrence P Ruggieri  
*University of Nevada, Las Vegas*

Follow this and additional works at: <https://digitalscholarship.unlv.edu/rtds>

---

### Repository Citation

Ruggieri, Lawrence P, "Update to ANSI/ANS-643-1991 for high-Z materials and review of particle transport theory" (2008). *UNLV Retrospective Theses & Dissertations*. 2427.  
<http://dx.doi.org/10.25669/x1i-qbff>

This Thesis is protected by copyright and/or related rights. It has been brought to you by Digital Scholarship@UNLV with permission from the rights-holder(s). You are free to use this Thesis in any way that is permitted by the copyright and related rights legislation that applies to your use. For other uses you need to obtain permission from the rights-holder(s) directly, unless additional rights are indicated by a Creative Commons license in the record and/or on the work itself.

This Thesis has been accepted for inclusion in UNLV Retrospective Theses & Dissertations by an authorized administrator of Digital Scholarship@UNLV. For more information, please contact [digitalscholarship@unlv.edu](mailto:digitalscholarship@unlv.edu).

UPDATE TO ANSI/ANS-6.4.3-1991 FOR HIGH-Z MATERIALS  
AND REVIEW OF PARTICLE TRANSPORT THEORY

by

Lawrence P. Ruggieri

Bachelor of Science, Mechanical Engineering  
University of Nevada, Las Vegas  
2006

A thesis submitted in partial fulfillment  
of the requirements for the

**Master of Science Degree in Mechanical Engineering  
Department of Mechanical Engineering  
Howard R. Hughes College of Engineering**

**Graduate College  
University of Nevada, Las Vegas  
December 2008**

UMI Number: 1463530

## INFORMATION TO USERS

The quality of this reproduction is dependent upon the quality of the copy submitted. Broken or indistinct print, colored or poor quality illustrations and photographs, print bleed-through, substandard margins, and improper alignment can adversely affect reproduction.

In the unlikely event that the author did not send a complete manuscript and there are missing pages, these will be noted. Also, if unauthorized copyright material had to be removed, a note will indicate the deletion.

**UMI**<sup>®</sup>

---

UMI Microform 1463530

Copyright 2009 by ProQuest LLC.

All rights reserved. This microform edition is protected against unauthorized copying under Title 17, United States Code.

ProQuest LLC  
789 E. Eisenhower Parkway  
PO Box 1346  
Ann Arbor, MI 48106-1346



## Thesis Approval

The Graduate College  
University of Nevada, Las Vegas

November 25, 2008

The Thesis prepared by

Lawrence P. Ruggieri

Entitled

Update to ANSI/ANS-6.4.3-1991 for High-Z Materials

and Review of Particle Transport Theory

is approved in partial fulfillment of the requirements for the degree of

Master of Science in Engineering

Examination Committee Chair

Dean of the Graduate College

Examination Committee Member

Examination Committee Member

Graduate College Faculty Representative

## ABSTRACT

### **Update to ANSI/ANS-6.4.3-1991 for High-Z Materials and Review of Particle Transport Theory**

by

Lawrence P. Ruggieri

Dr. Charlotta Sanders, Examination Committee Co-Chair  
Professor of Nuclear Engineering  
University of Nevada, Las Vegas

Dr. Robert Boehm, Examination Committee Co-Chair  
Professor of Mechanical Engineering  
University of Nevada, Las Vegas

The ANSI/ANS-6.4.3-1991 Standard (ANSI/ANS-6.4.3, 1991), Gamma-Ray Attenuation Coefficients and Buildup Factors for Engineering Materials, presents evaluated gamma-ray elemental attenuation coefficients and single material buildup factors for selected engineering materials for use in shielding calculations. Since its last publication, new particle transport codes and cross-sectional data have become available. Therefore, this study was conducted for the purpose of updating gamma-ray buildup factors for high-Z materials that are presented in ANSI/ANS-6.4.3-1991 by using ENDF/B-VI.8 photo-atomic cross-section library data in MCNPX. The results from MCNPX were relatively in good agreement with those of ANSI/ANS-6.4.3-1991, which were calculated using PALLAS-1D (VII). A sample problem was run in both MCNPX and PALLAS and the results were in good agreement. New buildup factor and mass attenuation coefficient data tables are included in this paper along with the sample

calculation results used to compare MCNPX and PALLAS as well as the PHOTX and ENDF/B-VI.8 cross-section data libraries.

## TABLE OF CONTENTS

ABSTRACT.....	iii
ACKNOWLEDGEMENTS.....	vii
CHAPTER 1 INTRODUCTION .....	1
Purpose of the Study .....	1
Research Questions.....	1
Significance of the Study.....	2
Definition of Terms.....	3
Buildup Factors.....	6
Buildup Factor Calculations .....	6
Boltzmann Transport Equation .....	10
Integral Form of the Transport Equation .....	11
PALLAS-1D (VII).....	12
MCNPX.....	14
Some Differences between PALLAS-1D (VII) and MCNPX.....	15
Photon Interactions .....	16
Cross-Section Data Libraries .....	16
CHAPTER 2 REVIEW OF RELATED LITERATURE.....	18
Literature Review.....	18
CHAPTER 3 METHODOLOGY .....	22
Literature Review Criteria .....	22
Computations .....	22
Fitting Functions .....	27
CHAPTER 4 FINDINGS OF THE STUDY.....	28
Analysis of Data.....	28
CHAPTER 5 SUMMARY, CONCLUSIONS, AND RECOMMENDATIONS.....	31
Discussion of Results.....	31
Conclusions.....	32
Recommendations for further Study.....	33
REFERENCES .....	35

APPENDICES .....	38
Appendix I     Photon Mass Attenuation Coefficients for Lead Coherent Scattering Not Included .....	39
Appendix II    Photon Mass Attenuation Coefficients for Lead Coherent Scattering Included .....	40
Appendix III   Absorbed Dose Response Functions for Lead .....	41
Appendix IV    Comparison of PHOTX and ENDF/B-VI.8 in PALLAS-1D (VII) .....	42
Appendix V     Comparison of PALLAS-1D (VII) and MCNPX Using ENDF/B-VI.8 Data .....	43
Appendix VI    MCNPX Energy Absorption Buildup Factor Compared to ANS-6.4.3-1991 .....	44
Appendix VII   PALLAS-1D (VII) Sample Input File .....	75
Appendix VIII  MCNPX Sample Input File.....	76
VITA .....	79



## ACKNOWLEDGEMENTS

I would like to acknowledge Dr. Charlotta Sanders for her guidance, patience, and continued support. She was my guiding light through this study and its completion would not have been possible without her. I could not have asked for a better mentor. I am also thankful to Marc Sanders, J.D., whose patience and flexibility were above and beyond all expectations. I would also like to thank Drs. Robert Boehm, Brendan O'Toole, and John Mercer for their interest in my research and participating in my advisory committee.

I would like to thank Dr. Evgeny Stankovskiy for his contributions to this project, especially his help with getting PALLAS up and running as well as MCNPX support. Many thanks to Dr. Jeff Ryman who helped develop and shape this project. I would like to thank Dr. Denis Beller for his support and suggestions.

I would like to acknowledge and thank my friends and colleagues Luis Durani and Kamran Haq who have been instrumental to this study and supportive in many areas. Special thanks to Dr. Yukio Sakamoto, Dr. Yoshiko Harima, Dr. Dermott "Red" Cullen, Mike Herman, Ramon Arcilla Jr., Dr. Michael Dunn, Dr. Nicholas Tsoulfanidis, Adam Davis, and Dr. Jabo Tang. I have been overwhelmed by the kindness, graciousness, and intelligence of these individuals. They have provided much needed information, tribal knowledge, and guidance that was beyond my expectations. Their willingness to help has been more than admirable and I am indebted to them.

I would like to thank Varian Medical Systems for their support in furthering my education and completing this study. I would like to acknowledge Richard LaFave, Dr. Gongyin Chen, and Douglas Eaton of Varian Medical Systems for supporting me through this process. They have been generous with their time and knowledge and have made me laugh when I needed it most. I would especially like to thank my supervisor, colleague, mentor, and good friend, John Stammetti, who has been a role model to me. I have enjoyed the many personal conversations that we have had as well as the professional ones.

I would like to thank my parents for always pushing me to do my best and further my education.

Lastly, I would like to thank my wife and our beautiful daughters. I love them dearly and thank them for the sacrifices they have made and the love and support they have given me.

## CHAPTER 1

### INTRODUCTION

#### Purpose of the Study

The ANSI/ANS-6.4.3-1991 Standard (ANSI/ANS-6.4.3, 1991), Gamma-Ray Attenuation Coefficients and Buildup Factors for Engineering Materials, (to be herein referred to as ANS Standard) presents evaluated gamma-ray elemental attenuation coefficients and single material buildup factors for selected engineering materials for use in shielding calculations. Since the publication of the ANS Standard, new cross-sectional data has become available. The current status of the ANSI/ANS-6.4.3-1991 is “withdrawn” due to the failure to meet the requirement of the American Nuclear Society to have standards updated every ten years to be considered active documents. The ANS Standard may become active again and shed its withdrawn status if it is updated. Therefore, this study was conducted for the purpose of updating gamma-ray buildup factors for high-Z engineering materials that are presented in the current ANS Standard. The information provided in the ANS Standard is often used in the nuclear industry for photon shielding applications, specifically, dose rate calculations. Having a current ANS Standard is essential to performing the most accurate analyses possible.

#### Research Questions

Understanding what has been previously done to generate buildup factors and generating new buildup factors is far from trivial. Certain questions must be asked to

develop meaningful results. The focus of this study was to answer the following questions.

1. How will the data generated in this study be useful to the ANSI/ANS-6.4.3 working group?
2. What are buildup factors and why are they important?
3. How are buildup factors calculated?
4. What is the transport equation and how is it used?
5. What methods were used to develop buildup factors for high Z-materials for the ANS Standard?
6. How do PALLAS-1D (VII) and MCNPX differ?
7. What effect will changing the cross-section data libraries used have on the results of the buildup factors?
8. How do the MCNPX results compare with the ANS Standard?

#### Significance of the Study

The buildup factor values that are provided in ANSI/ANS-6.4.3-1991 are derived from data that is at least seventeen years old. Within the last seventeen years new data have been generated to provide the nuclear community with more reliable values. Since 1991, computer technology has significantly improved, allowing for more complicated (detailed), computationally demanding codes to be utilized. Consequently, new codes model radiation transport more accurately than older codes. Providing new buildup factor data allows for validation of published values and may increase the accuracy of the information that is available. This study was performed for the ANS-6.4.3 working group as discussed by Ruggieri and Sanders (2008) and the results will be reviewed for

possible inclusion in the next revision of the ANS Standard. Providing more accurate data to the nuclear community can result in safer and possibly more cost effective designs. Ultimately, the values chosen for the ANS Standard will be the decided by the ANS working group. Traditionally, the ANS working group has chosen the values that were the most conservative for safety reasons.

#### Definition of Terms (Not Defined Elsewhere in this Study)

Absorption – Process in which photons, as they pass through a material, are absorbed in the material.

Annihilation photons – Positrons (positive electrons), generated either from the positron decay of radionuclides or from pair production interactions induced by high energy photons, lose energy as a result of collisions with atoms in the surrounding medium. After the positron has slowed down to very low energies, it combines with a negatron (negative electron), the two particles disappear, and two photons are produced. The two photons that are produced are the annihilation radiation or annihilation photons.

Attenuation – Combination of absorption and scattering processes in which photons, as they pass through material, are either stopped, or diverted from straight and forward travel. Total attenuation, depending on photon energy, is caused by photoelectric absorption, coherent and incoherent scattering, and pair production.

Bremsstrahlung – Bremsstrahlung, literally “braking radiation”, is the electromagnetic radiation emitted by a charged particle when it is rapidly decelerated by deflection in the electric field of an atom.

Compton scattering – Photon attenuation process in which a photon transfers part of its energy and momentum to an orbital electron of the attenuating material and continues to travel through the material at an angle to the original photon direction at a reduced energy.

Dose (Absorbed) – A measure of the amount of energy from an ionizing radiation deposited in a mass of some material.

Exposure (photon) – A radiation measurement quantity which is proportional to the electric charge of either sign that is created in air as a result of ionization by secondary charged particles resulting from photon interactions in a unit mass of air. (Shultis & Faw, 2000)

Fluorescence – The emission of characteristic secondary (or fluorescent) photons (X-rays) from atoms that have been excited by bombardment of high-energy (higher) X-rays or gamma-rays. The term is applied to phenomena in which the absorption of higher-energy radiation results in the re-emission of lower-energy radiation.

Isotropic radiation – Radiation which is emitted by a source in all directions with equal intensity, or which reaches a location from all directions with equal intensity.

Linear attenuation coefficient – Constant used to describe the degree of photon attenuation per unit path length in a specified medium. It is a function of particle energy and is usually expressed in units of  $\text{cm}^{-1}$ .

Pair production – An absorption process for photons of energies greater than 1.02 MeV, in which the photon transforms into a pair of particles (an electron and a positron).

Photoelectric absorption – An absorption process in which the photon loses all of its energy to an atomic electron. The electron leaves its atomic orbit and continues to move through the material.

Photon – The quantum of electromagnetic energy, regarded as a discrete particle having zero rest mass and no electric charge which travels in a vacuum at only the speed of light. Examples of photons in decreasing order of energy are gamma-rays, X-rays, ultraviolet light, visible light, and infrared light.

Point source – The most fundamental type of radiation source which is theoretical but is often used as an approximation to a real source provided that the real source's volume is sufficiently small compared to the volume of the attenuating medium and there is negligible interaction of radiation with the matter in the source volume. A point source

does not have any volume and is modeled as a point in space. In general, it can be characterized as being dependent on energy, direction, and time. (Shultis & Faw, 2000)

### Buildup Factors

The buildup factor is used in radiation calculations as a correction factor to account for effects that are not considered in calculations that use values for only uncollided particles. The buildup factor is defined as the ratio of the total value of a specified radiation quantity at any point to the contribution to that value from uncollided radiation as it relates to the passage of radiation through a medium. (Harima, 1993) For a point isotropic source of monoenergetic photons in an infinite homogeneous medium, it can be shown that the buildup factor depends spatially only on the number of mean free paths separating the source and the point of interest. The present study shall observe buildup factors in materials up to 40 mean-free-paths (mfp).

### Buildup Factor Calculations

Mean-free-path length is defined as the average distance  $\lambda$  that a radiation particle streams from the point of its birth to the point at which it makes its first interaction.

(Shultis & Faw, 2000) Mathematically, the mfp is described by the equation

$$\lambda = 1/\mu, \tag{1.1}$$

where  $\mu$  is the linear interaction coefficient or linear attenuation coefficient. The linear interaction coefficient can be described as the probability per unit path length of an interaction.  $\mu$  is always a function of the energy of the particle and can also be a function of the energy of the particle after scattering, the energy of the recoil atom or electron, the angles of deflection of the scattered radiation and the recoil atom or electron, and the angles of emission of secondary particles depending on the nature of the



interaction. This study focuses on photons, in particular gamma-rays, so when the term “energy” is used, it is meant as the total energy of the photon, which can be described by

$$E = h\nu, \quad (1.2)$$

where  $h$  is Planck’s constant and  $\nu$  is the frequency of the electromagnetic wave associated with the photon. In general, the linear interaction coefficient can be described by the equation

$$\mu = N \times \sigma \quad (1.3)$$

where  $N$  is the atomic density and  $\sigma$  is the microscopic cross-section. The atomic density  $N$  for a medium composed of a single element is

$$N = \frac{\rho}{A} \times N_a, \quad (1.4)$$

where  $A$  is the atomic mass of the element,  $\rho$  is the density of the element, and  $N_a$  is Avogadro’s number.

The microscopic cross-section,  $\sigma$ , is an effective cross-sectional area presented by the target atom or electron to the incident particle for a given interaction.  $\sigma$  has dimensions similar to those of physical area ( $\text{cm}^2$ ) but equivocating it to a physical area is not a very accurate analogy. The microscopic cross-section is material specific and is dependent upon the energy of the incident particle, and for a crystalline material, the particle direction. (Shultis & Faw, 2000) In radiation shielding calculations,  $\sigma$  is often drawn from a file known as a cross-section data library, which is a tabulation of microscopic cross-sections which are material specific and are dependent on the energy of the incident particle and type of interaction. The cross-section data library used in this study is

ENDF/B-VI.8, which is distributed by National Nuclear Data Center (NNDC), which is part of Brookhaven National Laboratory.

A form of the linear interaction coefficient commonly presented is the mass interaction coefficient, which is  $\frac{\mu}{\rho}$ . Once again  $\rho$  is the density of the medium in which the photon is traveling or interacting. In this study, mass interaction coefficients or more specifically, mass energy-absorption coefficients  $\left(\frac{\mu_{en}(E)}{\rho}\right)$ , are used in response function calculations. The response function or detector response provides an analytical relationship between fluence and dose. This study utilized two types of response functions: absorbed dose and exposure. The response function for absorbed dose, in units  $\text{Gy cm}^2$ , is

$$\mathfrak{R}_D(E) = 1.602 \times 10^{-10} E \left( \frac{\mu_{en}(E)}{\rho} \right), \quad (1.5)$$

which calculates the absorbed dose in the attenuating medium as a function of energy and is specific to the medium material. The exposure response function, in units  $\text{R cm}^2$ , is

$$\mathfrak{R}_X(E) = 1.835 \times 10^{-8} E \left( \frac{\mu_{en}(E)}{\rho} \right)_{air}, \quad (1.6)$$

which is proportional to the absolute value of the electric charge that is created in air as a result of ionization by secondary charged particles resulting from photon interactions in a unit mass of air.

To calculate dose or exposure, the respective response function is multiplied by the fluence at the location of interest or detector. The fluence,  $\Phi$ , is defined as the time-integrated flux of particles per unit area; usually from a pulse or burst of radiation.

(Lamarsh & Baratta, 2001) In this study, and in many other examples, the particle fluence can be thought of as the number of particles that, during some period of time, penetrate a spherical surface of interest. More specifically the term

$$\Phi^O(r) = \frac{S_p}{4\pi r^2} \quad (1.7)$$

is used to describe the uncollided fluence of particles from a distance,  $r$ , from the source; where  $s_p$  is the source strength (particles emitted per unit time). To calculate the uncollided dose from a point monoenergetic isotropic source embedded in an infinite homogenous medium characterized by the total interaction coefficient  $\mu$ ,

$$D^O(r) = \frac{S_p \mathfrak{R}_D}{4\pi r^2} e^{-\mu r}, \quad (1.8)$$

is used.  $e^{-\mu r}$  is referred to as the material attenuation term. The equation describing total dose is as follows:

$$D(r) = \int_{E_L}^{E_U} \Phi(E) \mathfrak{R}_D(E) dE, \quad (1.9)$$

where  $E_L$  is the lower energy boundary and  $E_U$  is the upper energy boundary.

(ANSI/ANS-6.1.1, 1991)

To calculate the energy absorption buildup factors for a particular material, the total dose is divided by the uncollided dose as shown:

$$B(r) \equiv \frac{D(r)}{D^O(r)}. \quad (1.10)$$

### Boltzmann Transport Equation (Transport Equation)

The transport equation is solved by integrating along a flight path of radiation in the direction of motion at each discrete-ordinate angle. (Harima, 1993) The most common basic form of the Boltzmann transport equation is as follows:

$$\Omega \cdot \nabla \phi(r, E, \Omega) + \mu(r, E) \phi(r, E, \Omega) = \int_0^\infty dE' \int_{4\pi} d\Omega' \mu_s(r, E' \rightarrow E, \Omega' \rightarrow \Omega) \phi(r, E', \Omega') + S(r, E, \Omega) \quad (1.11)$$

The form of the transport equation above is general and applies to any geometry, either photons or neutrons, and allows for all types of particle-medium interactions, all of whose probabilities are encompassed by the interaction coefficients  $\mu$  and  $\mu_s$ . It is known as an “integrodifferential” equation because it contains both derivatives in space and time as well as integrals over angle and energy. (Duderstadt, 1976) The above equation can be interpreted as follows. If  $V$  is an arbitrary control volume, then the net flow rate of the particles of the radiation field out of  $V$  across  $S$ , the surface of the volume, plus the rate at which particles interact in  $V$  is equal to the rate at which secondary particles of energy  $E$  and direction  $\Omega$  are produced (scattered) plus the rate of production of particles by sources in  $V$ .  $\phi$  is the fluence rate or flux density, which is the derivative with respect to time of the fluence.  $\mu(r, E) \phi(r, E, \Omega)$  is the “interaction term”, which describes the rate at which particles interact in the given volume.

$\int_0^\infty dE' \int_{4\pi} d\Omega' \mu_s(r, E' \rightarrow E, \Omega' \rightarrow \Omega) \phi(r, E', \Omega')$  is the “scattering term”, which describes the rate at which secondary particles of energy  $E$  and direction  $\Omega$  are produced.  $E'$  and  $\Omega'$  are used as initial energy and direction values while  $E$  and  $\Omega$  are used to describe the new energy and direction after scattering occurs.  $S(r, E, \Omega)$  is the “source term”, which

describes the rate of production by sources in the given volume. The “streaming term” of the equation, also known as leakage is  $\Omega \cdot \nabla \phi(r, E, \Omega)$ . (Duderstadt, 1976; Shultis & Faw, 2000) The leakage is generally the most difficult term to express because of geometry and coordinate system considerations. The above information is simply a review of the transport equation and is not meant to describe all of its forms or applications. A detailed description of the various forms and applications of the transport code is beyond the scope of this study and shall not be included.

The discretization of the transport equation is often accomplished by discrete ordinates methods. PALLAS uses a modified discrete ordinate approach known as the integral form of the transport equation. (Takeuchi & Tanaka, 1984; Takeuchi & Tanaka, 1981) The integral form of the transport equation can treat much more anisotropic radiation fields than can, for example, the standard multigroup discrete-ordinates method. (Shultis & Faw, 2000) A detailed discussion of the discrete ordinates method is outside of the scope of the present study and shall not be included.

### Integral Form of the Transport Equation

The steady-state version of the transport equation may be written

$$\frac{d}{dR} \phi(r, \Omega) dr d\Omega + \mu(r) \phi(r, \Omega) dr d\Omega = S(r, \Omega) dr d\Omega \quad (1.12)$$

where  $dR$  is the differential length along the direction  $\Omega$  (i.e.,  $\Omega \cdot \nabla = d / dR$ ). This equation may be integrated along the direction  $\Omega$  from  $r_0$  to  $r$ , to obtain

$$\phi(r, \Omega) dr = e^{-\alpha(r_0, r)} \phi(r_0, \Omega) dr_0 + \int_{r_0}^r e^{-\alpha(r', r)} S(r', \Omega) dr' \quad (1.13)$$

where  $\alpha(r', r)$  is the total number of mean-free path lengths along the direction  $\Omega$  between  $r'$  and  $r$  :

$$\alpha(r', r) \equiv \left| \int_{r'}^r \mu(R) dR \right|. \quad (1.14)$$

For an isotropic point source of strength  $S_0$  (particles/s) located at  $r_0$ , the directional flux outward through the cone  $d\Omega$  about direction  $\Omega$  is  $S_0(d\Omega/4\pi)$ . The volume element  $dr$  subtended by this cone at distance  $R = |r - r'|$  away is  $4\pi d\Omega R^2 dr$ . The directional flux at  $r$  of uncollided particles from an isotropic point source at  $r'$  (such that the direction from  $r'$  to  $r$  is  $\Omega$ ) is given by

$$\phi_{pt}(R) = \phi(|r - r'|, \Omega) = \frac{S_0 e^{-\alpha(r, r')}}{4\pi |r - r'|^2} = \frac{S_0 e^{-\alpha(R, 0)}}{4\pi R^2}. \quad (\text{Stacey, 2001}) \quad (1.15)$$

A detailed description of the various forms and applications of the integral transport equation is beyond the scope of this study and shall not be included.

### PALLAS-1D (VII)

PALLAS-1D (VII) uses the method of direct integration of the transport equation, in which the equation is integrated along the flight path of radiation in the direction of motion at each discrete ordinate direction. The radiation flux is calculated at each energy mesh ( $\text{n/cm}^2 \cdot \text{sec} \cdot (\text{sr}) \cdot \text{MeV}$ ) without using any conventional iterative techniques used widely in Sn (angular segmentation) method for obtaining group flux at each energy group and the scattering calculations are made directly using the Klein-Nishina formula for gamma-rays. The Klein-Nishina formula provides an approximation of incoherent scattering in which a differential cross-section is provided with respect to solid angle of scattering. Thus, a Legendre polynomial expansion approximation used widely in Sn method is not applied to the calculation of radiation scattering. As a result, PALLAS can provide always positive and physically meaningful angular and scalar fluxes. There is no

usage of an average flux. No convergence techniques are used for obtaining flux.

PALLAS-1D (VII) can treat transport of both neutrons and gamma-rays, in particular of secondary gamma-rays including the bremsstrahlung and the annihilation photons.

PALLAS was written in FORTRAN IV. The gamma-ray cross-sections are taken from the PALLAS gamma-ray library; however gamma-ray scattering cross-sections are not required due to the direct use of the Klein-Nishina formula. Coefficients for linear attenuation, pair production and photoelectric effect of gamma-rays are interpolated for specified energies from the PALLAS gamma-ray library in the code, where the data for discrete energies from 0.01 to 20 MeV are given. Similarly, the flux to dose conversion factor for exposure dose, dose equivalent and absorbed dose also are interpolated. The differential electron production cross-sections relating to the pair production reaction are calculated within the code. The differential bremsstrahlung gamma-ray production cross-sections and the stopping power are calculated within the code.

A disadvantage of PALLAS-1D (VII) code is that it has been written in the fixed dimensioning, which restricts the numbers of energy meshes, material regions, nuclides, angular meshes, spatial meshes to be inputted.

At the time of its initial release PALLAS used what was considered to be a new technique for treatment of the within-group scattering radiations instead of applying an iteration technique. The scattering within a certain small angle is approximated as being considered unscattered. PALLAS code calculates the within-group scattering radiations on the basis of this approximation.

## MCNPX

MCNPX is a general purpose Monte Carlo radiation transport code that tracks nearly all particles at nearly all energies. It is the next generation in the series of Monte Carlo transport codes that began at Los Alamos National Laboratory in the mid-20<sup>th</sup> century. The MCNPX program began in 1994 as an extension of MCNP4B and LAHET 2.8 in support of the Accelerator Production of Tritium Project (APT). (X-5 Monte Carlo Team, 2003)

Monte Carlo methods systematically use samples of random numbers to estimate parameters of an unknown distribution by statistical simulation. Monte Carlo methods are often used when the complexity or dimensionality of a problem is impossible or impractical to solve by conventional numerical solutions. The method is well-suited for computers and has become increasingly popular with advances in computer technology. There are advantages to using the Monte Carlo method for many applications; however, its disadvantages include potentially slow convergence and the difficulty of estimating the statistical error of the result(s).

The computational model for radiation transport problems includes geometry and material specifications. Object modeling is fundamental to perform photon transport effectively using the Monte Carlo method. Object modeling consists of defining geometry as well as assigning material characteristics to the volume of the object. The material characteristics of interest are the density and the interaction cross-sections. The Monte Carlo method's treatment of photo-atomic interactions is perhaps best described by Zaidi (2000): "The relative ratios of the cross-sections for photoelectric effect, incoherent and coherent scattering to the total cross-section are used to choose



randomly which process occurs at each interaction vertex. The Klein–Nishina expression for the differential cross-section per electron for an incoherent interaction is used to sample the energy and polar angle of the incoherently scattered photon taking into account the incoherent scattering factor. The coherent scattering results only in a change in the direction of the scattered photon since the momentum change is transferred to the whole atom. The random number composition and rejection technique is used to sample the momentum of the scattered photon and the scattering angle according to the form-factor distributions. Coherent scatter distributions are sharply forward-peaked and vary considerably with atomic number and energy. The path-length of the interacting photon is randomly generated according to the exponential attenuation based on the interaction length. The total cross-section at the energy of the interacting photon determines the interaction length of the exponential distribution.”

#### Some of the Differences between PALLAS-1D (VII) and MCNPX

Besides the obvious difference of MCNPX being a Monte Carlo method code and PALLAS being a code that directly integrates the transport equation, there are other differences in methodology between the codes. PALLAS uses linear interpolation while MCNPX uses logarithmic interpolation by default but can also use linear interpolation if prompted to do so. Typically, logarithmic interpolation is considered more accurate than linear interpolation in most radiation shielding calculations. A point source is treated exactly by MCNPX. Within PALLAS, the point source is modeled by specifying a source uniformly distributed on a spherical shell of small diameter.

### Photon Interactions

The majority of buildup-factor data is for point, isotropic, and monoenergetic sources of photons in infinite homogeneous media. Early data sets were based on moments-method calculations and accounted only for buildup of Compton-scattered photons. The buildup of annihilation photons was accounted for in subsequent moments-method calculations. Buildup-factor calculations using PALLAS code account for Compton-scattered photons, annihilation photons, and for fluorescence and bremsstrahlung. (Takeuchi & Tanaka, 1984; Takeuchi & Tanaka, 1981) Buildup factors in the ANS Standard exclude coherently scattered photons and treat Compton scattering according to the Klein-Nishina cross-section for photon scattering with free electrons. (ANSI/ANS-6.4.3, 1991; Shultis & Faw, 2000)

Dose to medium response functions used by PALLAS for the current ANS Standard shall be used in this study by both PALLAS and MCNPX; however, the cross-section data shall be from different sources. (ANSI/ANS-6.4.3, 1991; Takeuchi & Tanaka, 1984; Takeuchi & Tanaka, 1981)

### Cross-Section Data Libraries

Various cross-section data libraries are available for radiation transport computations. PHOTX cross-section data libraries (National Institute of Standards and Technology [NIST], n.d.) were used for the calculation of buildup factors for high-Z materials ( $Z=42$  thru  $Z=92$ ) that are listed in the ANS Standard. Originally, the PALLAS users chose Storm and Israel's (1970) data for their calculations; however, it had been discovered that the Hubbell's data (1969), NBS-29, and PHOTX data were more accurate; mostly due to their different method of treating Compton scattering. Since the publication of the ANS

Standard, new data libraries have been developed. Most notably, the ENDF formatted library collection has become adopted as the library format of choice in North America and other regions. Evaluated Nuclear Data File (ENDF) is a core nuclear reaction database containing evaluated cross-sections, spectra, angular distributions, fission product yields, thermal neutron scattering, photo-atomic and other data, with emphasis on neutron-induced reactions. (Chadwick et al., 2006) The ENDF formats and libraries are decided by the Cross-Section Evaluation Working Group (CSEWG), a cooperative effort of national laboratories, industry, and universities in the U.S. and Canada, and are maintained by the National Nuclear Data Center (NNDC). ENDF/B data sets are revised or replaced only after extensive review and testing.

## CHAPTER 2

### REVIEW OF RELATED LITERATURE

#### Literature Review

The accuracy of buildup factors has been debated since their inception. A lack of experiments and wide range of results from numerical solutions make it difficult to identify the most accurate data. The necessity of using a monoenergetic source is the single biggest constraint that is in the way of gathering more data via experiments. As discussed by Harima (1993), experiments by White, Osanev et al., Miyasaka and Tsuruo, Takeuchi and Tanaka, Furuta et al., Tamura and Tsuruo, and Ahmed et al. have used Co-60 and Cs-137 sources; however, these two sources do not provide enough source energies to conduct a comprehensive analysis of experimental data versus data from simulated models. According to Harima (1993), there were fairly large differences between some measured and calculated results. Not only are there disagreements in results between measured and calculated results, there is also disagreement between the calculated results themselves. Harima (1993) states that even if the fluxes of energy spectra and the values of buildup factors agree within tolerable deviations between different codes at distances close to the source, differences become large at deep depths, and it is difficult to determine which code is correct. The differences in the codes have often been due to assumptions made in the calculations rather than mathematical differences by themselves. In a study by Subbaiah et al. (1982), the significance of

secondary sources of photons as a result of annihilation, bremsstrahlung, and fluorescence in gamma-ray transport calculations is discussed in detail. Prior to the study, most computations were performed using Compton-scattered sources only and annihilation, bremsstrahlung, and fluorescence were not taken into account. For low atomic number materials and low energy gamma-rays where the effects of secondary sources are marginal, this assumption can arguably be appropriate. However, when high-Z materials or high energy photons are being studied, this assumption is not valid and calculation results would be significantly inaccurate. In 1987, Subbaiah and Natarajan (1987) revisited the effects of fluorescence in buildup factor calculations but his time explored the effect in deep penetration of gamma rays. Their study revealed that the inclusion of fluorescence leads to a spectacular increase in buildup factors for source energies close to but above the K edge of the medium. The increase was observed to grow with depth of penetration. Harima et al. (1991) studied the buildup factors of high-Z materials with energies near the K edge. The K edge in lead is 0.0880045 MeV. Fluorescence can account for an increase in the buildup factor by as much as a factor of 10 for source energies near the K edge; however, the great change in photoelectric cross-sections dominates in this energy range and results in a rapid increase of the buildup factor in the order of  $10^{14}$  ( $10^{12}$  for lead in ANS Standard). The large values gradually lower with increasing energy above the K edge until reaching values that are “normal” at 0.16 MeV.

Takeuchi and Tanaka (1984, 1981) also sought to increase the accuracy of their calculations by including bremsstrahlung and annihilation, which was previously missing from their previous revision of PALLAS (PL,SP-Br). Many studies conducted prior to

the ANS Standard's release neglected coherent scattering. The argument for neglecting coherent scattering is that it does not lead to the degradation of the energy of the photon and is very forward directed. (Goldstein, 1954) Subbaiah et al. (1989) found that inclusion of coherent scattering in calculations is necessary and that data that had been generated by methods which excluded coherent scattering was inaccurate and could be corrected by adding a correction factor or recalculating the values with coherent scattering. Harima et al. (1987) examined the error of the buildup factor due to the use of different cross-section data libraries. In particular, the photoelectric cross-section values of Hubbell's compilation (1969), Storm and Israel's data (1970) and ENDF/B (Chadwick, 2006) were compared and fairly large differences were observed. The buildup factor steeply rises as the source energy approaches the K edge and discontinuously falls at the K edge. According to Tanaka and Takeuchi (1986), to obtain more accurate results for buildup factors in deep penetration, more accurate cross-section data are necessary. It is estimated that the uncertainty of the cross-section for the energy region where the photoelectric absorption is dominant is approximately 10%. Shimizu (2004) confirmed that the variation of the photoelectric cross-section has a profound effect on the results of buildup factor calculations. Shimizu (2004) observed discrepancies in the values generated by the method of invariant embedding compared to the ANS Standard for high-Z materials in the energy range above 1.5 MeV and in the vicinity of the K edge. Shimizu (2004) argues that the discrepancies are a result of the modeling of secondary photons. The calculations for the ANS Standard used the assumption that all secondary photons are emitted in the same direction as the primary photon. The magnitude of the discrepancy appears to increase with source energy. 10%

to 30% difference is seen in the vicinity of the K edge for all high-Z materials. Shimizu (2004) only provided exposure buildup factors but stated that the energy absorption buildup factors would be reported in the near future, but as of November 2008, the energy absorption buildup factors are not found in the literature. Chibani (2001) observed that at 10 MeV and above, discrepancies between the ANSI Standard and the values generated by the EBUF Monte Carlo method code for lead were significant. Bozkurt and Tsoulfanidis (1996) were successful at calculating buildup factors for  $\text{UO}_2$  up to 10 mfp using MCNP; however, they did not report whether or not they attempted to calculate buildup factors for greater than 10 mfp.

## CHAPTER 3

### METHODOLOGY

#### Literature Review Criteria

Select articles referenced in the ANS Standard as well as more recent articles found within the WEB OF SCIENCE database was researched for relevant data. The literature found within the WEB OF SCIENCE was limited to English language publications between 1991 and 2008. Articles that were chosen to be included in this review were chosen based on pre-established inclusion criteria.

Inclusion criteria are as follows:

- Source is peer-reviewed journal or similar scholarly publication
- Discusses gamma-ray buildup factors, photon transport equation, PALLAS-1D, MCNP, MCNPX, and/or ANSI/ANS-6.4.3-1991.
- Publication occurred between 1991 and 2008 or is referenced in ANS Standard.

Sources of data, computer codes used, methodology, and results were reviewed for each article. Textbooks and online sources of data were used in addition to the scholarly articles. The online sources of data were restricted to government or government related organizations such as national laboratories and international organizations.

#### Computations

This study focuses on gamma-ray buildup factor values for high-Z materials. The materials listed in the ANS Standard that are considered high-Z are Mo, Sn, La, Gd, W,



Pb, and U. PALLAS data were used exclusively for the buildup factor calculations of high-Z materials in the ANS Standard. (ANSI/ANS-6.4.3, 1991) The techniques used in this study to calculate buildup factors may be applied to all of the aforementioned high-Z materials; however, lead (Pb) was the focus of this study. Consistent with the ANS Standard, point, isotropic, and monoenergetic sources of photons in infinite homogeneous media were modeled using MCNPX and PALLAS codes, respectively.

Photon mass attenuation coefficients ( $\text{cm}^2/\text{g}$ ) with and without coherent scattering were calculated using ENDF/B-VI.8 photo-atomic interaction cross-sections for energies within the range of .010 to 30.000, which are consistent with the ANS Standard. Not only are these values included in the ANS Standard, they are also necessary for the calculation of mean-free path values. A comparison between the new ENDF/B-VI.8 photon mass attenuation coefficients and those of the ANS Standard for lead without and with coherent scattering are provided in Appendix I and Appendix II, respectively.

In the current ANS Standard, the gamma-ray buildup factors for high-Z materials were generated by PALLAS-1D (VII) code using PHOTX cross-section libraries. (ANSI/ANS-6.4.3, 1991; Takeuchi & Tanaka, 1984) Early on in this study it was decided that ENDF/B-VII.0 would be the library of choice for generating new data. ENDF/B-VII.0 was chosen because it is the latest version of ENDF/B to be officially released. However, after researching the ENDF/B-VII.0 data, it was found that the photo-atomic interaction data for ENDF/B-VII.0 is identical to what is found in ENDF/B-VI.8. The photo-atomic interaction data used in ENDF/B-VI.8 are that of EPDL97 (Evaluated Photon interaction Data Library – 1997). (Cullen, 1997) ENDF/B-VI.8 was the first version of ENDF/B to use EPDL97 data, while the previous release used the data of

EPDL89. The photo-atomic interaction data were not updated since the release of EPDL97 because there has not been much demand from the nuclear community. ENDF/B-VI.8 photo-atomic data was used in this study because it is equivalent to ENDF/B-VII.0 and because the ENDF/B-VI.8 ACE-formatted (ASCII) files are readily available whereas ENDF/B-VII.0 ACE-formatted files for photo-atomic interactions are not available.

To study the effects of using the ENDF/B-VI.8 photo-atomic data instead of the PHOTX data, a sample problem, shown in Appendix VII, was run in PALLAS with both PHOTX and ENDF/B-VI.8 data for photo-atomic interactions. The ENDF/B-VI.8 data were converted into a format that is readable by PALLAS through elementary equations which convert cross-sections (barns) to attenuation coefficients ( $\text{cm}^2/\text{g}$ ). Table 4 of Appendix IV shows the percentage difference between the PHOTX data and the ENDF/B-VI.8 data at each energy value. Mass energy-absorption and mass energy-transfer coefficients using ENDF/B-VI.8 (or ENDF/B-VII.0) data were not found. To provide mass energy coefficient values that are more current than those previously used, data from the National Institute of Standards and Technology (Hubbell & Seltzer, 2004) (n.d.) were used. The NIST values were used directly in the PALLAS data library.

To study the effects of using two different computational codes, the PALLAS sample problem was duplicated in MCNPX using the ENDF/B-VI.8 data, which is given in the data library, mcplib04, which is provided by the Radiation Safety Information Computational Center (RSICC) with MCNPX. The NIST values for the mass energy coefficients were used indirectly in MCNPX via the dose card which incorporates the NIST data in its derivation. Ideally, ENDF/B-VI.8 values would be used for the mass

energy coefficients to be consistent; however, ENDF/B-VI.8 mass energy coefficients are not yet available and the NIST values are the most current that were found. The results from the sample problem using ENDF/B-VI.8 data in PALLAS and ENDF/B-VI.8 in MCNPX were compared and are shown in Table 5 of Appendix V.

After examining some of the differences between ENDF/B-VI.8 and PHOTX and MCNPX and PALLAS, MCNPX was used to calculate a new table of buildup factors for lead (Pb). The energies examined were the same as those used in the ANS Standard; ranging from 0.03MeV up to 15 MeV. Elemental lead (Pb) was chosen as the material of interest and mfp thickness values from 0.5 to 40 were used, which is consistent with what had been done in the ANS Standard. All mfp values were calculated using the total microscopic cross-section data from ENDF/B-VI.8. An isotropic monoenergetic point source was used in all input files. The variance reduction technique known as importance mapping, specifically geometry splitting (Los Alamos National Laboratory [LANL], 2005), was used to improve statistics. Hirayama (1995) found that particle splitting is an effective variance reduction technique for calculation of buildup factors up to 40 mfp using the Monte Carlo method. Total absorbed dose and uncollided absorbed dose calculations were performed simultaneously by the use of energy bins. The same method may be used for total exposure and uncollided exposure calculations. Absorbed dose card values were calculated using NIST values and can be seen in Table 3 of Appendix III. The values used in the absorbed dose cards are for the energy range of .001 MeV through 20 MeV and are logarithmically interpolated when values fall between the discrete values that are given in the cards. To provide acceptable statistics without excessively long run times,  $10^6$  source particle histories were run for each input card. In a few instances where

the source energy was either near the k-edge energy range or above 10 MeV, more source particle histories were run to improve results. Due to the number of mean-free-paths used, surface tallies were used to calculate fluence rather than point detectors or ring detectors. Next event estimators such as point and ring detectors are known to be unreliable when calculating the fluence at large numbers of mean-free-paths in scattering medium. If next event estimators are used, the user risks under-sampling coherent scattering which is characterized by many low scores to the detector when the photon trajectory is away from the detector and a very few, enormously large scores when the trajectory is nearly aimed at the detector. Such under-sampled events cause a sudden increase in both the tally and the variance, and a failure to pass the statistical checks for the tally. (X-5 Monte Carlo Team, 2003) Concentric spheres were used with the point source located at the origin (0 0 0). The radii of the spheres were assigned mfp values. Additional spheres were added between mfp values to ensure that the difference in importance between cells never exceeded a factor of four. The thickness of the material extended beyond 40 mfp and then became a void to simulate an infinite homogeneous medium. An example of an input file used to calculate the total absorbed dose and uncollided absorbed dose is included in Appendix VIII. Once all of the desired values for total and uncollided dose were calculated, those values were used to calculate their respective buildup factors.

The values generated by MCNPX were compared with the published values (PALLAS) in the ANS Standard and are provided in Tables 6a through 6ae of Appendix VI. MCNPX was chosen to be the primary code used for this study because it is currently supported by the Radiation Safety Information Computational Center (RSICC) and is

widely used by professionals in the nuclear industry whereas PALLAS is unsupported and there are currently no known users. PALLAS has been included in the study for use as a comparative tool and to provide a starting point for the transition to a more current code (MCNPX).

### Fitting Functions

Generated buildup factor data are commonly fitted to curves to provide a method of determining buildup factor values that fall between generated data points. Buildup factor coefficients using both geometric progression and Taylor fitting function coefficients were presented in data tables in the ANS Standard. Consistent with the ANS Standard, the data generated by MCNPX shall be curve fitted using geometric progression and Taylor fitting function coefficients or similar techniques. (ANSI/ANS-6.4.3, 1991) Curve fitting shall be completed by members of the ANS-6.4.3 working group and shall not be included in this study. The values generated by MCNPX shall be compared with the published values in the ANS Standard

## CHAPTER 4

### FINDINGS OF THE STUDY

#### Analysis of Data

There was a maximum percentage difference of 1.14% (at 0.080 MeV) and a minimum percentage difference of 0.01% (at 20.000 MeV) between the ENDF/B-VI.8 photon mass attenuation coefficients with coherent scattering for lead, which was used to calculate mfp values for MCNPX, compared to those of the ANS Standard.

There was a maximum percentage difference of 2.01% (at 0.080 MeV) and a minimum percentage difference of 0.04% (at 30.000 MeV) between the ENDF/B-VI.8 photon mass attenuation coefficients without coherent scattering for lead, which was used to calculate mfp values for MCNPX, compared to those of the ANS Standard.

There was a maximum percentage difference of 12.86% (at 10.0 mfp) and a minimum percentage difference of 0.16% (at 3.0 mfp) between the energy absorption buildup factors calculated in the PALLAS sample problem using ENDF/B-VI.8 and PHOTX cross-section data libraries, respectively.

There was a maximum percentage difference of 13.36% (at 10.0 mfp) and a minimum percentage difference of 2.93% (at 0.5 mfp) between the energy absorption buildup factors calculated in PALLAS and MCNPX using ENDF/B-VI.8 data library cross-sections.

The percentage difference in the range of 0.500 to 40.000 mean-free paths at various energies in the range of 0.03 MeV to 15.000 MeV were calculated to compare the energy absorption buildup factors calculated in MCNPX with those of the ANS Standard. The maximum and minimum percentage differences are shown in Table A. The energy absorption buildup factors calculated within MCNPX and from the ANS Standard are provided along with their percentage differences in Tables 6a through 6ae in Appendix VI. At certain mean-free path lengths for particular source energies, buildup factors could not be calculated using MCNPX data.

**Table A** Maximum and Minimum Percentage Differences between MCNPX and the ANS Standard at Each Source Energy

Energy (MeV)	MCNPX Maximum % Difference	mfp Value of Maximum % Difference	MCNPX Minimum % Difference	mfp Value of Minimum % Difference	Max mfp Value Buildup Factor Obtained
0.030	16.04%	1.000	12.95%	35.000	40.000
0.040	10.86%	0.500	7.20%	40.000	40.000
0.050	8.07%	1.000	3.93%	40.000	40.000
0.060	6.71%	0.500	1.33%	35.000	40.000
0.080	5.02%	40.000	0.14%	8.000	40.000
0.088	8.54%	40.000	0.64%	1.000	40.000
0.089	33.93%	1.000	1.92%	7.000	25.000
0.090	32.58%	1.000	0.57%	10.000	35.000
0.100	85.90%	20.000	3.06%	15.000	25.000
0.110	46.23%	25.000	2.92%	5.000	30.000
0.120	46.42%	30.000	0.56%	6.000	35.000
0.130	42.12%	40.000	0.68%	7.000	40.000
0.140	15.74%	0.500	2.63%	8.000	40.000
0.150	14.28%	1.000	0.85%	15.000	40.000
0.160	13.66%	0.500	2.62%	40.000	40.000
0.200	8.69%	0.500	0.84%	20.000	40.000
0.300	5.07%	0.500	0.30%	15.000	40.000
0.400	11.20%	40.000	0.04%	6.000	40.000
0.500	12.46%	40.000	0.02%	5.000	40.000
0.600	13.43%	0.500	4.29%	40.000	40.000
0.800	12.32%	7.000	6.44%	40.000	40.000
1.000	10.94%	5.000	5.02%	40.000	40.000
1.500	12.74%	0.500	0.26%	20.000	40.000
2.000	11.71%	5.000	7.03%	40.000	40.000
3.000	20.44%	40.000	5.33%	0.500	40.000
4.000	35.49%	40.000	5.55%	0.500	40.000
5.000	15.25%	15.000	1.97%	0.500	40.000
6.000	29.63%	40.000	1.83%	0.500	40.000
8.000	22.35%	40.000	0.36%	0.500	40.000
10.000	53.65%	40.000	0.17%	8.000	40.000
15.000	38.78%	30.000	1.27%	10.000	35.000



## CHAPTER 5

### SUMMARY, CONCLUSIONS, AND RECOMMENDATIONS

#### Discussion of Results

The photon mass attenuation coefficients derived from ENDF/B-VI.8 for the case when coherent scattering is considered as well as the case where coherent scattering is ignored showed surprisingly good agreement with the values of the ANS Standard. The percentage difference between the values was relatively small (2.01% or less); however, these relatively small differences can produce large differences in the final results. Perhaps the clearest example of the effect that the differences in mass attenuation coefficients is the PALLAS sample problem results where both libraries' values were used but no other variables were modified. There was up to a 12.86% difference in values and the study only went to 10.0 mfp. It is expected that the difference would become greater with increase in mfp because of the stack-up of differences in values.

The 13.36% difference at 10.0 mfp between PALLAS and MCNPX when both codes used the ENDF/B-VI.8 values demonstrates that the solution methods of the codes themselves cause results to vary. Some of these differences can be accounted for in the physics models used by each code while others are probably due to differences in the computational techniques.

For the most part, the energy absorption buildup factors calculated in MCNPX had good agreement (<10%) with those of the ANS Standard. There were large relative

errors for values near the k-edge energy range as well as at 15 MeV at deep mean-free path lengths. The large relative errors can at least partially be explained by the stack-up of uncertainty as particles scatter within the medium and travel to deeper mfp depths. Near the K-edge energy range there is a significant increase in the photoelectric cross-section. The increase in the photoelectric cross-section is proportional to an increase in the number of interactions. There is uncertainty associated with each interaction and with more interactions comes more uncertainty. Due to the large relative errors, some buildup factors could not be calculated. Buildup factors could not be calculated when the uncollided dose value is equal to zero. MCNPX generated uncollided dose values of zero which would indicate that there were issues with the results. The calculation method used was suggested and reviewed by some of the active members of the X-5 Monte Carlo team, known experts. They suggested that the number of particle histories be increased to resolve the zero flux issue. This was done but did not significantly improve the results. They had no other immediate suggestions. Becoming an expert user of Monte Carlo codes was not part of the scope of this study and no further attempts were made at improving the results for these problematic cases. Should additional studies be conducted using MCNPX to generate buildup factor data, new techniques and/or methods should be implemented to resolve the current issues. There were no general trends noticed in the calculated values except that on average the MCNPX values were greater than those of the ANS Standard.

### Conclusions

Updating the ANS Standard buildup factors using current cross-section libraries provides nuclear professionals with more accurate data and serves well as a verification

of previously published data. Increased buildup factor accuracy enables nuclear professionals to design safer structures and may result in decreased cost of new shielding designs. The differences between the energy absorption buildup factors calculated in this study and those of the ANS Standard can easily be explained by differences in cross-section data libraries, calculation methods, and physics assumptions. While some inaccuracies were observed in the new data, it is believed that most of the new values (other than those previously noted as being inaccurate) are more accurate than those published in the ANS Standard. MCNPX performs calculations with much greater detail and resolution than PALLAS. The combination of using more a detailed computational code with more accurate cross-section data than was used in the ANS Standard justifies the proposed use of the data in ANS Standard.

#### Recommendations for further Study

It is essential to the success of the newest revision of the ANS Standard that mass energy-absorption and mass energy-transfer coefficients from ENDF/B-VI.8 data be calculated. Seltzer's method (1993) should be reviewed to see if it is applicable for use with ENDF/B-VI.8 cross-sections. Calculation of these values from ENDF/B-VI.8 will provide the most accurate data available for buildup factor calculations and consequently will increase the accuracy of results as well as show good consistency in the calculation method. When new mass energy-absorption and mass energy-transfer coefficients that are derived from ENDF/B-VI.8 (EPDL97) data become available, the calculations performed in this study should be repeated to improve their consistency and accuracy. Curve fitting should be performed using geometric progression or Taylor fitting function coefficients or both.

A comparison between the data from this study should be made with data from recent studies (studies performed after the 1991 ANS Standard was published) which include new codes such as EBUF (a new Monte Carlo code) and new methods of calculating buildup factors such as the Method of Invariant Embedding and the Angular Eigenvalue Method. (Chibani, 2001; Shimizu, 2004; Shimizu, 2000)

Data should be generated for some of the “new” shielding materials that are not included in the ANS Standard. Many of these “new” materials are used in the medical industry and it would be of great value to have them added to the ANS Standard. Examples of “new” materials include tungsten polymers and high density concretes.

Recently, much work has been focused on layered shields. The ANS working group should consider adding values for layered shields or approximation methods to the next revision of the ANS Standard.

## REFERENCES

1. **ANSI/ANS-6.1.1-1991**, *American National Standard for Neutron and Gamma-Ray Fluence-to-Dose Factors*, American Nuclear Society, La Grange Park (1991)
2. **ANSI/ANS-6.4.3-1991**, *Gamma-Ray Attenuation Coefficients and Buildup Factors for Engineering Materials*, American Nuclear Society, La Grange Park (1991)
3. **Bozkurt A**, Tsoulfanidis N. Exposure Buildup Factors of  $\text{UO}_2$  Using the Monte Carlo Method. *Nuclear Technology* 1996;116:257-260
4. **Chadwick M**, Oblozinsky P, Herman M, *et al.* ENDF/B-VII.0: Next Generation Evaluated Nuclear Data Library For Nuclear Science and Technology. *Nuclear Data Sheets* 2006;107:2931-3060
5. **Chibani O**. New Photon Exposure Buildup Factors. *Nuclear Science and Engineering* 2001;137:215-225
6. **Cullen D**, Hubbell J, *et al.* "The Evaluated Photon Data Library, '97 version," *UCRL-50400*, Vol. 6, Rev. 5 (1997).
7. **Duderstadt J**, Hamilton L. (1976). *Nuclear Reactor Analysis* (1st ed.). New York: John Wiley & Sons, Inc.
8. **Goldstein H**, Wilkins J. Calculations of the Penetration of Gamma Rays. *Nuclear Development Associates, Inc.* 1954;NYO-3075
9. **Harima Y**. An Historical Review and Current Status of Buildup Factor Calculations and Applications. *Radiation Physics and Chemistry* 1993;41:631-672
10. **Harima Y**, Trubey D, *et al.* Gamma-Ray Attenuation in the Vicinity of the K Edge in Molybdenum, Tin, Lanthanum, Gadolinium, Tungsten, Lead, and Uranium. *Nuclear Science and Engineering* 1991;107:385-393
11. **Harima Y**, Hirayama H, *et al.* A Comparison of Gamma-Ray Buildup Factors for Low-Z Material and for Low Energies Using Discrete Ordinates and Point Monte Carlo Methods. *Nuclear Science and Engineering* 1987;96:241-252
12. **Hirayama H**. Calculation of Gamma-ray Exposure Buildup Factors up to 40 mfp using the EGS4 Monte Carlo Code with a Particle Splitting. *Journal of Nuclear Science and Technology* 1995;32:1201-1207

13. **Hubbell J, Seltzer S.** Tables of X-Ray Mass Attenuation Coefficients and Mass Energy-Absorption Coefficients (version 1.4). 2004 [Online] Available: <http://physics.nist.gov/xaamdi> [2008, November 3]. National Institute of Standards and Technology, Gaithersburg, MD.
14. **Hubbell J.** Photon Cross-sections, Attenuation Coefficients, and Energy Absorption Coefficients from 10 keV to 100 GeV," NSRDS-NBS-29, National Standard Reference Data Systems, U.S. National Bureau of Standards (1969).
15. **Lamarsh J, Baratta A.** (2001). *Introduction to Nuclear Engineering* (3rd ed.). New Jersey: Prentice-Hall, Inc.
16. **LANL** (Regents of the University of California at Los Alamos National Laboratory). MCNPX User's Manual, Version 2.5.0, **LA-CP-05-0369**, Los Alamos National Laboratory, Los Alamos (2005).
17. **NIST** (National Institute of Standards and Technology). PHOTX: Photon Interaction Cross-Sections, **DLC-136**, Radiation Shielding Information Center Data Package
18. **Ruggieri L, Sanders, C.** Update to ANSI/ANS-6.4.3-1991 Gamma-Ray Buildup Factors for High-Z Engineering Materials (Part I). *Trans. Am. Nucl. Soc.*, 99, November 2008
19. **Seltzer S.** Calculation of Photon Mass Energy-Transfer and Mass Energy-Absorption Coefficients. *Radiation Research* 1993;136:147-170
20. **Shimizu A, Onda T, et al.** Calculation of Gamma-Ray Buildup Factors up to Depths of 100 mfp by the Method of Invariant Embedding, (III) Generation of an Improved Data Set. *Nuclear Science and Technology* 2004;41:413-424
21. **Shimizu A.** Development of Angular Eigenvalue Method for Radiation Transport Problems in Slabs and Its Application to Penetration of Gamma-rays. *Nuclear Science and Technology* 2000;37:15-25
22. **Shultis K, Faw R.** (2000). *Radiation Shielding* (1st ed.). Illinois: American Nuclear Society, Inc.
23. **Stacey W.** (2001). *Nuclear Reactor Physics* (1st ed.). New York: John Wiley & Sons, Inc.
24. **Storm E, Israel H.** Photon Cross-Sections from 1keV to 100 MeV for Elements Z=1 to Z=100. *Nuclear Data Tables* 1970;A7:565

25. **Subbaiah K**, Natarajan A, *et al.* Impact of Coherent Scattering on the Spectra and Energy Deposition of Gamma Rays in Bulk Media. *Nuclear Science and Engineering* 1989;101:352-370
26. **Subbaiah K**, Natarajan A, *et al.* Effect of Fluorescence in Deep Penetration of Gamma Rays. *Nuclear Science and Engineering* 1987;96:330-342
27. **Subbaiah K**, Natarajan A, *et al.* Effect of Fluorescence, Bremsstrahlung, and Annihilation Radiation on the Spectra and Energy Deposition of Gamma-rays in Bulk Media. *Nuclear Science and Engineering* 1982;81:172-195
28. **Tanaka S**, Takeuchi K. Detailed Investigation of the Buildup Factors and Spectra for Point Isotropic Gamma-Ray Sources in the Vicinity of the K Edge in Lead. *Nuclear Science and Engineering* 1986;93:376-385
29. **Takeuchi K**, Tanaka S. PALLAS-PL,SP-Br: A Code for Direct Integration of Transport Equation in One-Dimensional Plane and Spherical Geometries. *JAERI-M 84-214: Japan Atomic Energy Research Institute* 1984;84-214:1-77
30. **Takeuchi K**, Tanaka S. PALLAS-PL,SP-Br: A Code for Direct Integration of Transport Equation in One-Dimensional Plane and Spherical Geometries. *JAERI-M 9695: Japan Atomic Energy Research Institute* 1981;9695:1-87
31. **X-5 Monte Carlo Team**. MCNP – A General Monte Carlo N-Particle Transport Code, Version 5, Los Alamos National Laboratory, Los Alamos (2003).
32. **Zaidi H**. Comparative Evaluation of Photon Cross-Section Libraries for Materials of Interest in PET Monte Carlo Simulations. *IEEE Transactions on Nuclear Science* 2000;77:2722-2735

## APPENDICES



# APPENDIX I

**Table 1** Photon Mass Attenuation Coefficients for Lead  
Coherent Scattering Not Included

Energy (MeV)	MCNPX Photon Mass Attenuation Coefficient (cm <sup>2</sup> /g)	ANS-6.4.3-1991 Photon Mass Attenuation Coefficient (cm <sup>2</sup> /g) (Lead)	% Difference
0.010	1.256E+02	1.257E+02	0.08%
0.015	1.088E+02	1.084E+02	0.35%
0.020	8.374E+01	8.411E+01	0.44%
0.030	2.892E+01	2.900E+01	0.26%
0.040	1.343E+01	1.349E+01	0.41%
0.050	7.383E+00	7.426E+00	0.58%
0.060	4.528E+00	4.563E+00	0.77%
0.080	2.111E+00	2.135E+00	1.14%
0.100	5.356E+00	5.356E+00	0.02%
0.150	1.912E+00	1.921E+00	0.48%
0.200	9.372E-01	9.432E-01	0.63%
0.300	3.738E-01	3.772E-01	0.89%
0.400	2.151E-01	2.172E-01	0.98%
0.500	1.500E-01	1.514E-01	0.92%
0.600	1.169E-01	1.178E-01	0.79%
0.800	8.403E-02	8.472E-02	0.81%
1.000	6.798E-02	6.844E-02	0.67%
1.500	5.093E-02	5.102E-02	0.17%
2.000	4.524E-02	4.536E-02	0.28%
3.000	4.204E-02	4.199E-02	0.12%
4.000	4.172E-02	4.175E-02	0.06%
5.000	4.254E-02	4.257E-02	0.07%
6.000	4.386E-02	4.379E-02	0.14%
8.000	4.674E-02	4.667E-02	0.14%
10.000	4.964E-02	4.965E-02	0.01%
15.000	5.658E-02	5.653E-02	0.09%
20.000	6.201E-02	6.202E-02	0.01%
30.000	7.022E-02	7.019E-02	0.05%

## APPENDIX II

**Table 2**      **Photon Mass Attenuation Coefficients for Lead**  
**Coherent Scattering Included**

Energy (MeV)	MCNPX Photon Mass Attenuation Coefficient (cm <sup>2</sup> /g)	ANS-6.4.3-1991 Photon Mass Attenuation Coefficient (cm <sup>2</sup> /g) (Lead)	% Difference
0.010	1.299E+02	1.306E+02	0.55%
0.015	1.113E+02	1.116E+02	0.29%
0.020	8.601E+01	8.637E+01	0.42%
0.030	3.029E+01	3.032E+01	0.10%
0.040	1.433E+01	1.436E+01	0.24%
0.050	8.001E+00	8.041E+00	0.50%
0.060	4.979E+00	5.020E+00	0.81%
0.080	2.370E+00	2.419E+00	2.01%
0.100	5.545E+00	5.549E+00	0.07%
0.150	2.006E+00	2.015E+00	0.42%
0.200	9.958E-01	9.986E-01	0.28%
0.300	4.012E-01	4.032E-01	0.49%
0.400	2.310E-01	2.323E-01	0.58%
0.500	1.603E-01	1.613E-01	0.61%
0.600	1.239E-01	1.248E-01	0.69%
0.800	8.813E-02	8.870E-02	0.65%
1.000	7.064E-02	7.102E-02	0.54%
1.500	5.197E-02	5.222E-02	0.49%
2.000	4.590E-02	4.606E-02	0.35%
3.000	4.221E-02	4.234E-02	0.31%
4.000	4.188E-02	4.197E-02	0.21%
5.000	4.264E-02	4.272E-02	0.18%
6.000	4.383E-02	4.391E-02	0.18%
8.000	4.669E-02	4.675E-02	0.13%
10.000	4.967E-02	4.972E-02	0.10%
15.000	5.653E-02	5.658E-02	0.08%
20.000	6.202E-02	6.206E-02	0.07%
30.000	7.019E-02	7.022E-02	0.04%

# APPENDIX III

Table 3 Absorbed Dose Response Functions for Lead

Energy (MeV)	Photon Mass Energy-Absorption Coefficient (cm <sup>2</sup> /g) (NIST)	Absorbed Dose Response Function (Gy*cm <sup>2</sup> ) (Shielding Text 5.26)
0.001	5.197E+03	8.326E-10
0.0015	2.344E+03	5.633E-10
0.002	1.274E+03	4.082E-10
0.003	1.913E+03	9.194E-10
0.004	1.221E+03	7.824E-10
0.005	7.124E+02	5.706E-10
0.006	4.546E+02	4.370E-10
0.008	2.207E+02	2.828E-10
0.010	1.247E+02	1.998E-10
0.015	9.100E+01	2.187E-10
0.020	6.899E+01	2.210E-10
0.030	2.536E+01	1.219E-10
0.040	1.211E+01	7.760E-11
0.050	6.740E+00	5.399E-11
0.060	4.149E+00	3.988E-11
0.080	1.916E+00	2.456E-11
0.100	1.976E+00	3.166E-11
0.150	1.056E+00	2.538E-11
0.200	5.870E-01	1.881E-11
0.300	2.455E-01	1.180E-11
0.400	1.370E-01	8.779E-12
0.500	9.128E-02	7.312E-12
0.600	6.819E-02	6.554E-12
0.800	4.644E-02	5.952E-12
1.000	3.654E-02	5.854E-12
1.500	2.640E-02	6.344E-12
2.000	2.360E-02	7.561E-12
3.000	2.322E-02	1.116E-11
4.000	2.449E-02	1.569E-11
5.000	2.600E-02	2.083E-11
6.000	2.744E-02	2.638E-11
8.000	2.989E-02	3.831E-11
10.000	3.181E-02	5.096E-11
15.000	3.478E-02	8.358E-11
20.000	3.595E-02	1.152E-10

# APPENDIX IV

Table 4 Comparison of PHOTX and ENDF/B-VI.8 in PALLAS-1D (VI)

Energy (MeV)	mfp (Lead)	PHOTX Energy Absorption Buildup Factor	ENDF/B-VI.8 Energy Absorption Buildup Factor	% Difference
15	0.5	1.3220E+00	1.3116E+00	0.79%
15	1.0	1.5299E+00	1.5146E+00	1.00%
15	2.0	1.9096E+00	1.9008E+00	0.46%
15	3.0	2.4334E+00	2.4372E+00	0.16%
15	4.0	3.1588E+00	3.1997E+00	1.29%
15	5.0	4.1660E+00	4.2794E+00	2.72%
15	10.0	1.7439E+01	1.9681E+01	12.86%

## APPENDIX V

**Table 5 Comparison of PALLAS-1D (VII) and MCNPX Using ENDF/B-VI.8 Data**

<b>Energy (MeV)</b>	<b>mfp (Lead)</b>	<b>PALLAS Energy Absorption Buildup Factor</b>	<b>MCNPX Energy Absorption Buildup Factor</b>	<b>% Difference</b>
15	0.5	1.3116E+00	1.3500E+00	2.93%
15	1.0	1.5146E+00	1.5800E+00	4.32%
15	2.0	1.9008E+00	2.0500E+00	7.85%
15	3.0	2.4372E+00	2.6900E+00	10.37%
15	4.0	3.1997E+00	3.5500E+00	10.95%
15	5.0	4.2794E+00	4.4700E+00	4.45%
15	10.0	1.9681E+01	2.2310E+01	13.36%

## APPENDIX VI

**Table 6a**      **MCNPX Energy Absorption Buildup Factor Compared to ANS-6.4.3-1991**

Energy (MeV)	mfp (Lead)	Energy Absorption Buildup Factor New	Energy Absorption Buildup Factor ANS-6.4.3-1991	% Difference
0.03	0.500	1.16	1.01	15.05%
0.03	1.000	1.17	1.01	16.04%
0.03	2.000	1.16	1.01	15.26%
0.03	3.000	1.16	1.01	14.63%
0.03	4.000	1.15	1.01	14.29%
0.03	5.000	1.16	1.01	14.46%
0.03	6.000	1.15	1.01	14.32%
0.03	7.000	1.16	1.01	14.46%
0.03	8.000	1.16	1.02	13.25%
0.03	10.000	1.15	1.02	12.99%
0.03	15.000	1.16	1.02	13.47%
0.03	20.000	1.16	1.02	13.38%
0.03	25.000	1.15	1.02	13.21%
0.03	30.000	1.16	1.02	13.31%
0.03	35.000	1.15	1.02	12.95%
0.03	40.000	1.16	1.02	13.52%

**Figure 6a**

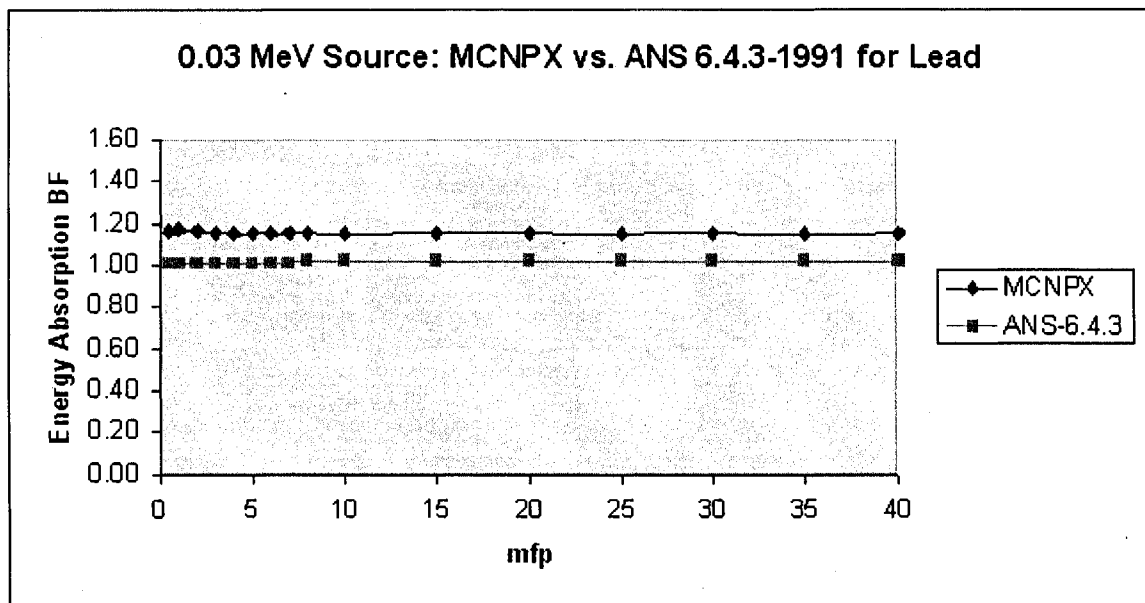


Table 6b MCNPX Energy Absorption Buildup Factor Compared to ANS-6.4.3-1991

Energy (MeV)	mfp (Lead)	Energy Absorption Buildup Factor New	Energy Absorption Buildup Factor ANS-6.4.3-1991	% Difference
0.04	0.500	1.12	1.01	10.86%
0.04	1.000	1.12	1.01	10.66%
0.04	2.000	1.12	1.02	9.67%
0.04	3.000	1.12	1.02	9.84%
0.04	4.000	1.12	1.02	9.84%
0.04	5.000	1.12	1.02	9.92%
0.04	6.000	1.12	1.03	8.92%
0.04	7.000	1.12	1.03	8.96%
0.04	8.000	1.12	1.03	9.07%
0.04	10.000	1.12	1.03	8.95%
0.04	15.000	1.12	1.04	7.90%
0.04	20.000	1.12	1.04	7.86%
0.04	25.000	1.13	1.04	8.20%
0.04	30.000	1.12	1.04	8.02%
0.04	35.000	1.13	1.05	7.21%
0.04	40.000	1.13	1.05	7.20%

Figure 6b

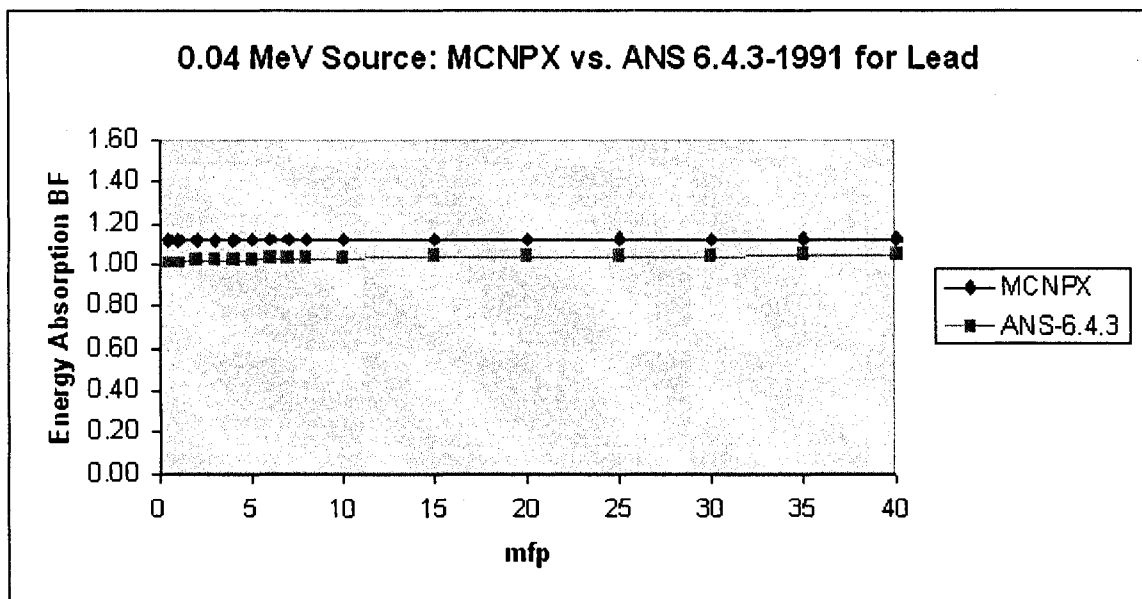


Table 6c MCNPX Energy Absorption Buildup Factor Compared to ANS-6.4.3-1991

Energy (MeV)	mfp (Lead)	Energy Absorption Buildup Factor New	Energy Absorption Buildup Factor ANS-6.4.3-1991	% Difference
0.05	0.500	1.10	1.02	7.55%
0.05	1.000	1.10	1.02	8.07%
0.05	2.000	1.10	1.03	7.21%
0.05	3.000	1.11	1.04	6.63%
0.05	4.000	1.11	1.04	6.90%
0.05	5.000	1.11	1.04	6.94%
0.05	6.000	1.11	1.05	5.63%
0.05	7.000	1.11	1.05	5.85%
0.05	8.000	1.11	1.05	6.05%
0.05	10.000	1.12	1.05	6.26%
0.05	15.000	1.12	1.06	5.53%
0.05	20.000	1.12	1.06	5.54%
0.05	25.000	1.12	1.07	4.65%
0.05	30.000	1.12	1.07	4.88%
0.05	35.000	1.12	1.08	4.08%
0.05	40.000	1.12	1.08	3.93%

Figure 6c

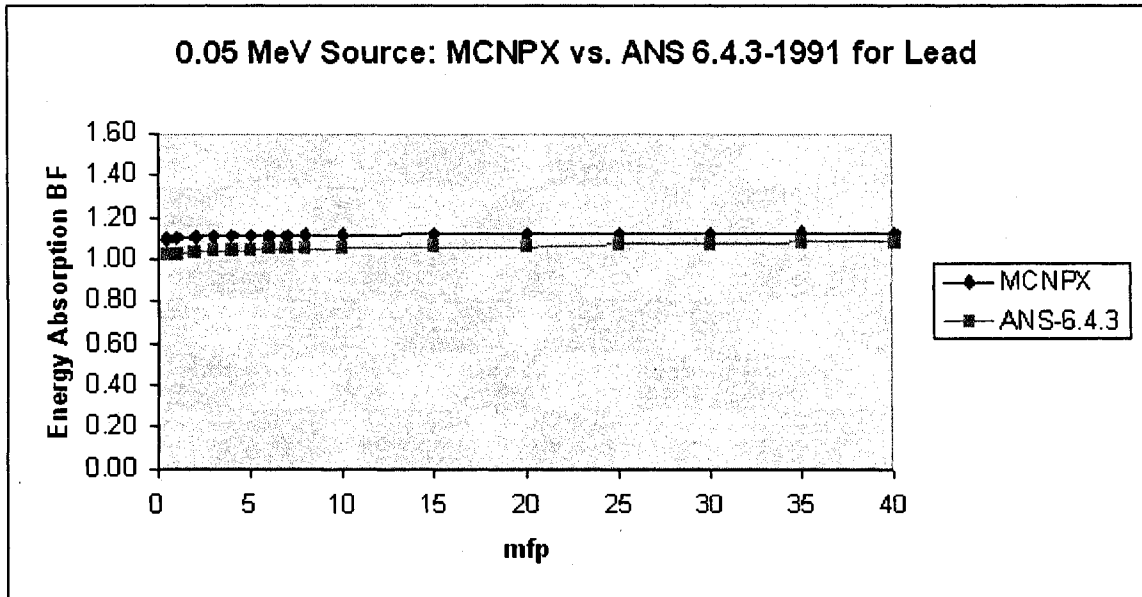




Table 6d MCNPX Energy Absorption Buildup Factor Compared to ANS-6.4.3-1991

Energy (MeV)	mfp (Lead)	Energy Absorption Buildup Factor New	Energy Absorption Buildup Factor ANS-6.4.3-1991	% Difference
0.06	0.500	1.09	1.02	6.71%
0.06	1.000	1.10	1.04	5.60%
0.06	2.000	1.10	1.05	5.20%
0.06	3.000	1.11	1.06	4.82%
0.06	4.000	1.11	1.06	4.78%
0.06	5.000	1.11	1.06	4.91%
0.06	6.000	1.11	1.07	4.06%
0.06	7.000	1.12	1.07	4.62%
0.06	8.000	1.12	1.08	3.95%
0.06	10.000	1.13	1.08	4.38%
0.06	15.000	1.13	1.09	3.40%
0.06	20.000	1.13	1.10	2.52%
0.06	25.000	1.13	1.11	1.81%
0.06	30.000	1.14	1.11	2.32%
0.06	35.000	1.13	1.12	1.33%
0.06	40.000	1.14	1.12	1.51%

Figure 6d

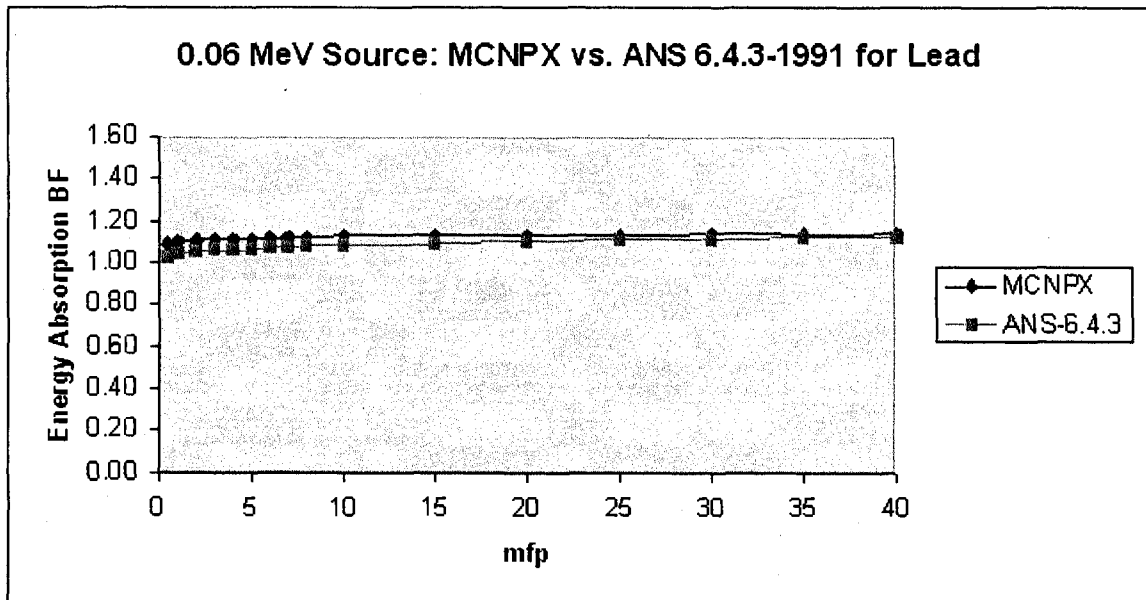


Table 6e MCNPX Energy Absorption Buildup Factor Compared to ANS-6.4.3-1991

Energy (MeV)	mfp (Lead)	Energy Absorption Buildup Factor New	Energy Absorption Buildup Factor ANS-6.4.3-1991	% Difference
0.08	0.500	1.10	1.05	4.29%
0.08	1.000	1.11	1.08	2.73%
0.08	2.000	1.13	1.10	2.94%
0.08	3.000	1.14	1.11	2.27%
0.08	4.000	1.14	1.12	2.16%
0.08	5.000	1.15	1.13	1.70%
0.08	6.000	1.15	1.14	1.15%
0.08	7.000	1.16	1.15	0.62%
0.08	8.000	1.16	1.16	0.14%
0.08	10.000	1.17	1.17	0.36%
0.08	15.000	1.18	1.19	1.21%
0.08	20.000	1.18	1.21	2.12%
0.08	25.000	1.19	1.22	2.68%
0.08	30.000	1.20	1.24	3.38%
0.08	35.000	1.20	1.25	4.12%
0.08	40.000	1.20	1.26	5.02%

Figure 6e

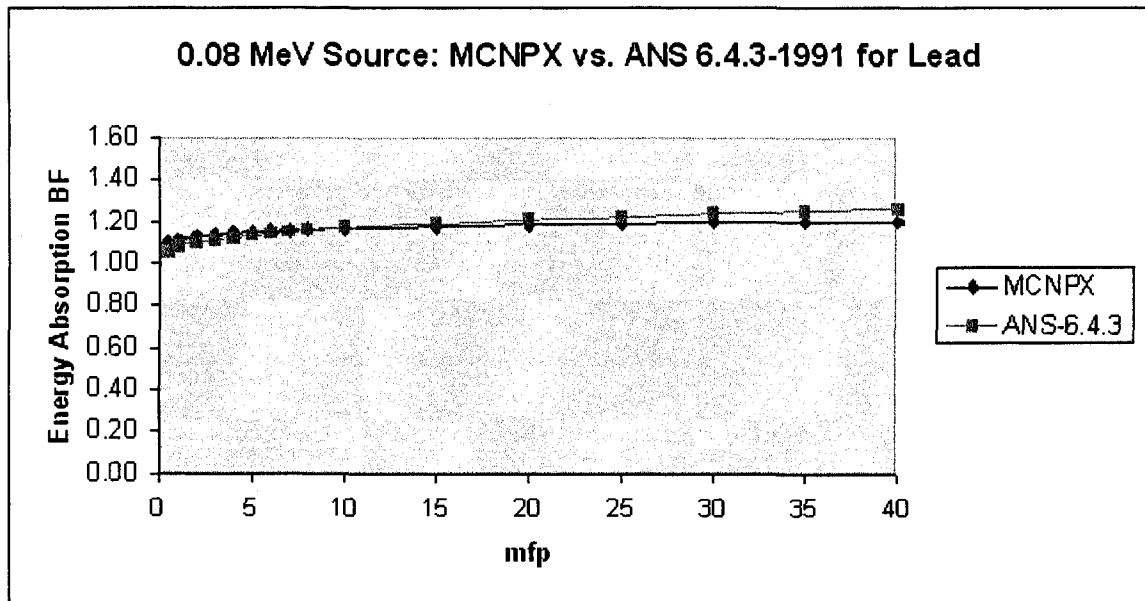


Table 6f MCNPX Energy Absorption Buildup Factor Compared to ANS-6.4.3-1991

Energy (MeV)	mfp (Lead)	Energy Absorption Buildup Factor New	Energy Absorption Buildup Factor ANS-6.4.3-1991	% Difference
0.088	0.500	1.08	1.07	0.82%
0.088	1.000	1.09	1.10	0.64%
0.088	2.000	1.11	1.12	0.71%
0.088	3.000	1.13	1.14	1.30%
0.088	4.000	1.13	1.15	1.60%
0.088	5.000	1.14	1.16	1.60%
0.088	6.000	1.15	1.18	2.80%
0.088	7.000	1.15	1.19	3.19%
0.088	8.000	1.16	1.19	2.75%
0.088	10.000	1.16	1.21	3.92%
0.088	15.000	1.18	1.24	4.97%
0.088	20.000	1.18	1.26	6.00%
0.088	25.000	1.19	1.28	6.79%
0.088	30.000	1.20	1.30	7.88%
0.088	35.000	1.21	1.31	7.97%
0.088	40.000	1.21	1.32	8.54%

Figure 6f

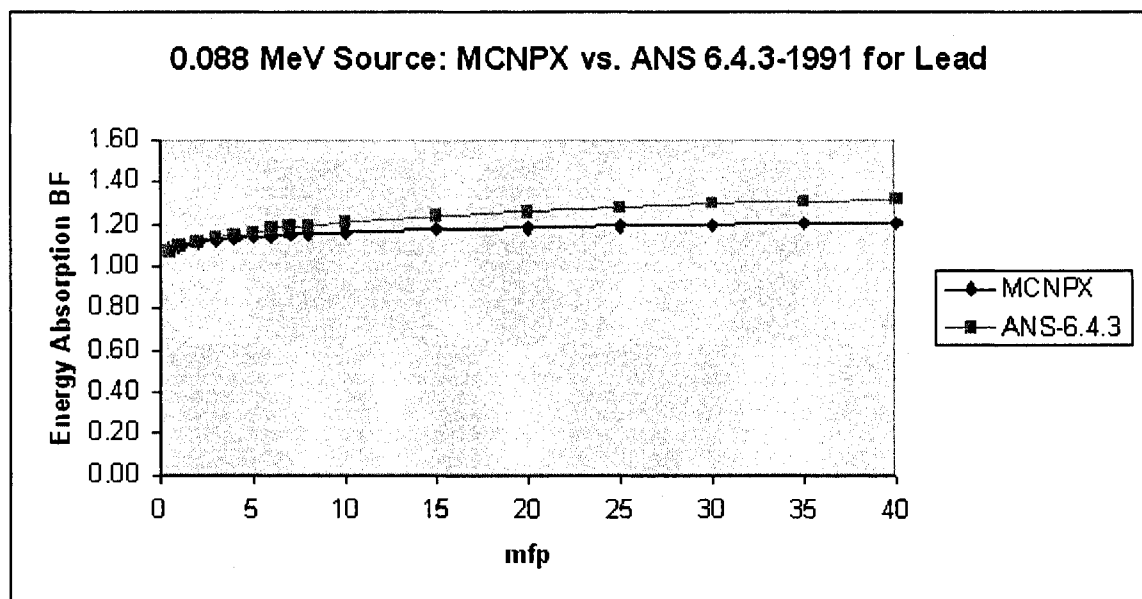


Table 6g MCNPX Energy Absorption Buildup Factor Compared to ANS-6.4.3-1991

Energy (MeV)	mfp (Lead)	Energy Absorption Buildup Factor New	Energy Absorption Buildup Factor ANS-6.4.3-1991	% Difference
0.089	0.500	1.93	1.48	30.52%
0.089	1.000	2.69	2.01	33.93%
0.089	2.000	4.71	3.54	33.00%
0.089	3.000	8.19	6.39	28.17%
0.089	4.000	1.46E+01	1.22E+01	19.84%
0.089	5.000	2.66E+01	2.41E+01	10.50%
0.089	6.000	4.99E+01	4.85E+01	2.96%
0.089	7.000	9.56E+01	9.38E+01	1.92%
0.089	8.000	1.83E+02	1.79E+02	2.47%
0.089	10.000	6.98E+02	6.71E+02	4.08%
0.089	15.000	2.41E+04	2.00E+04	20.57%
0.089	20.000	8.83E+05	6.71E+05	31.54%
0.089	25.000	* NO VALUE	2.44E+07	
0.089	30.000	* NO VALUE	9.36E+08	
0.089	35.000	* NO VALUE	3.74E+10	
0.089	40.000	* NO VALUE	1.53E+12	

\* The relative error in MCNPX was very high and Uncollided Dose was equal to zero

Figure 6g

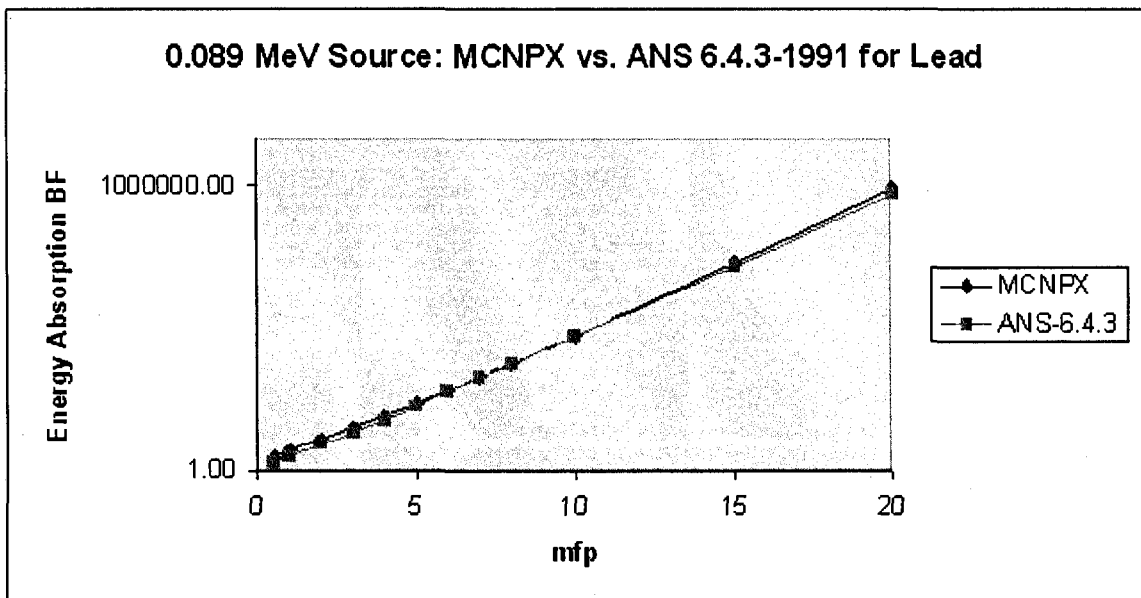


Table 6h MCNPX Energy Absorption Buildup Factor Compared to ANS-6.4.3-1991

Energy (MeV)	mfp (Lead)	Energy Absorption Buildup Factor New	Energy Absorption Buildup Factor ANS-6.4.3-1991	% Difference
0.090	0.500	1.91	1.48	29.10%
0.090	1.000	2.65	2.00	32.58%
0.090	2.000	4.62	3.49	32.30%
0.090	3.000	7.93	6.24	27.10%
0.090	4.000	1.39E+01	1.18E+01	18.04%
0.090	5.000	2.51E+01	2.31E+01	8.72%
0.090	6.000	4.63E+01	4.59E+01	0.90%
0.090	7.000	8.68E+01	8.78E+01	1.09%
0.090	8.000	1.65E+02	1.66E+02	0.77%
0.090	10.000	6.08E+02	6.11E+02	0.57%
0.090	15.000	1.73E+04	1.75E+04	1.22%
0.090	20.000	5.25E+05	5.66E+05	7.27%
0.090	25.000	1.45E+07	1.99E+07	26.97%
0.090	30.000	7.86E+08	7.40E+08	6.24%
0.090	35.000	*NO VALUE	2.86E+10	
0.090	40.000	*NO VALUE	1.13E+12	

\* The relative error in MCNPX was very high and Uncollided Dose was equal to zero

Figure 6h

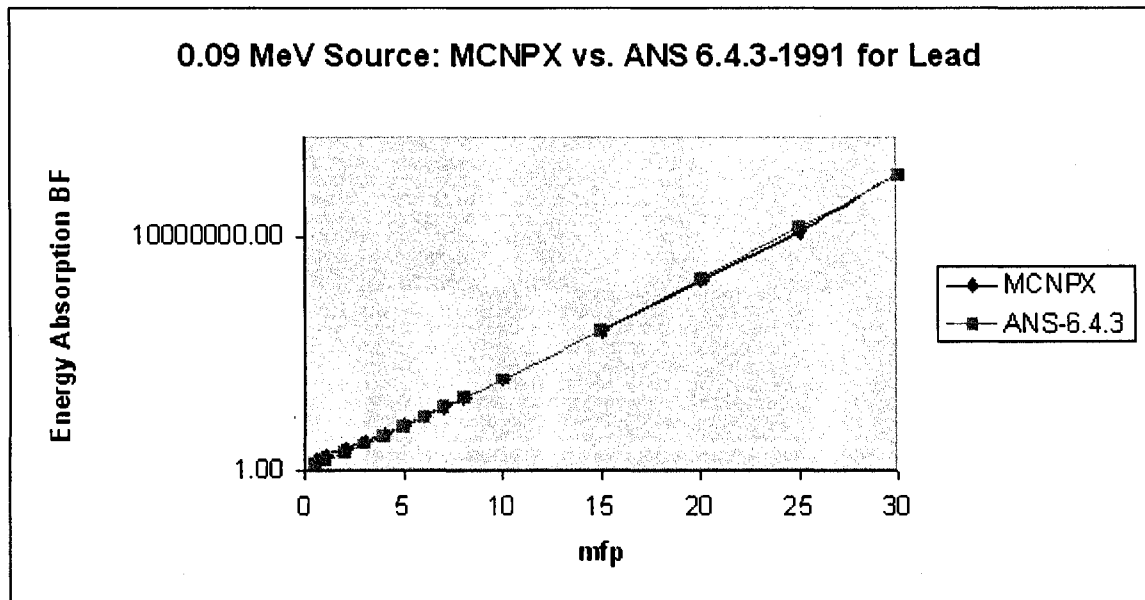


Table 6i MCNPX Energy Absorption Buildup Factor Compared to ANS-6.4.3-1991

Energy (MeV)	mfp (Lead)	Energy Absorption Buildup Factor New	Energy Absorption Buildup Factor ANS-6.4.3-1991	% Difference
0.100	0.500	1.75	1.44	21.22%
0.100	1.000	2.33	1.89	23.39%
0.100	2.000	3.73	3.05	22.40%
0.100	3.000	5.81	4.92	18.13%
0.100	4.000	9.18	8.25	11.23%
0.100	5.000	1.48E+01	1.44E+01	3.10%
0.100	6.000	2.45E+01	2.54E+01	3.64%
0.100	7.000	4.16E+01	4.50E+01	7.58%
0.100	8.000	7.15E+01	7.67E+01	6.82%
0.100	10.000	2.18E+02	2.32E+02	6.01%
0.100	15.000	4.46E+03	4.33E+03	3.06%
0.100	20.000	1.77E+05	9.54E+04	85.90%
0.100	25.000	*NO VALUE	2.33E+06	
0.100	30.000	*NO VALUE	6.02E+07	
0.100	35.000	*NO VALUE	1.61E+09	
0.100	40.000	*NO VALUE	4.35E+10	

\* The relative error in MCNPX was very high and Uncollided Dose was equal to zero

Figure 6i

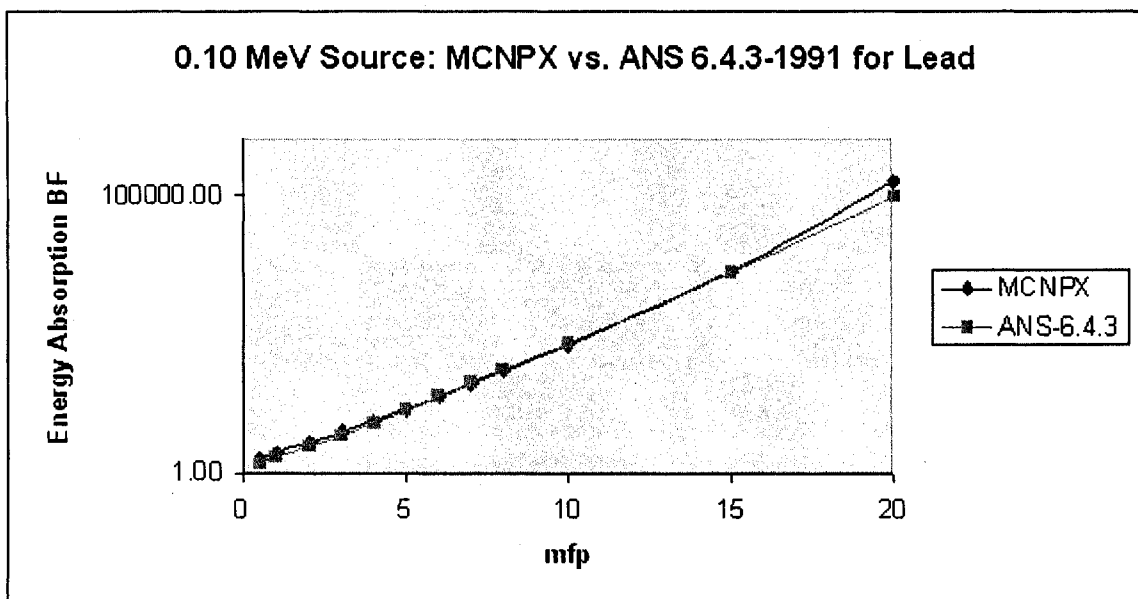


Table 6j MCNPX Energy Absorption Buildup Factor Compared to ANS-6.4.3-1991

Energy (MeV)	mfp (Lead)	Energy Absorption Buildup Factor New	Energy Absorption Buildup Factor ANS-6.4.3-1991	% Difference
0.110	0.500	1.73	1.45	19.19%
0.110	1.000	2.27	1.88	20.98%
0.110	2.000	3.40	2.85	19.37%
0.110	3.000	4.86	4.20	15.70%
0.110	4.000	6.92	6.30	9.79%
0.110	5.000	9.99	9.71	2.92%
0.110	6.000	1.47E+01	1.52E+01	3.08%
0.110	7.000	2.19E+01	2.41E+01	9.20%
0.110	8.000	3.37E+01	3.77E+01	10.70%
0.110	10.000	8.37E+01	9.20E+01	9.03%
0.110	15.000	1.02E+03	1.08E+03	5.37%
0.110	20.000	1.09E+04	1.55E+04	29.96%
0.110	25.000	1.34E+05	2.49E+05	46.23%
0.110	30.000	*NO VALUE	4.19E+06	
0.110	35.000	*NO VALUE	7.20E+07	
0.110	40.000	*NO VALUE	1.25E+09	

\* The relative error in MCNPX was very high and Uncollided Dose was equal to zero

Figure 6j

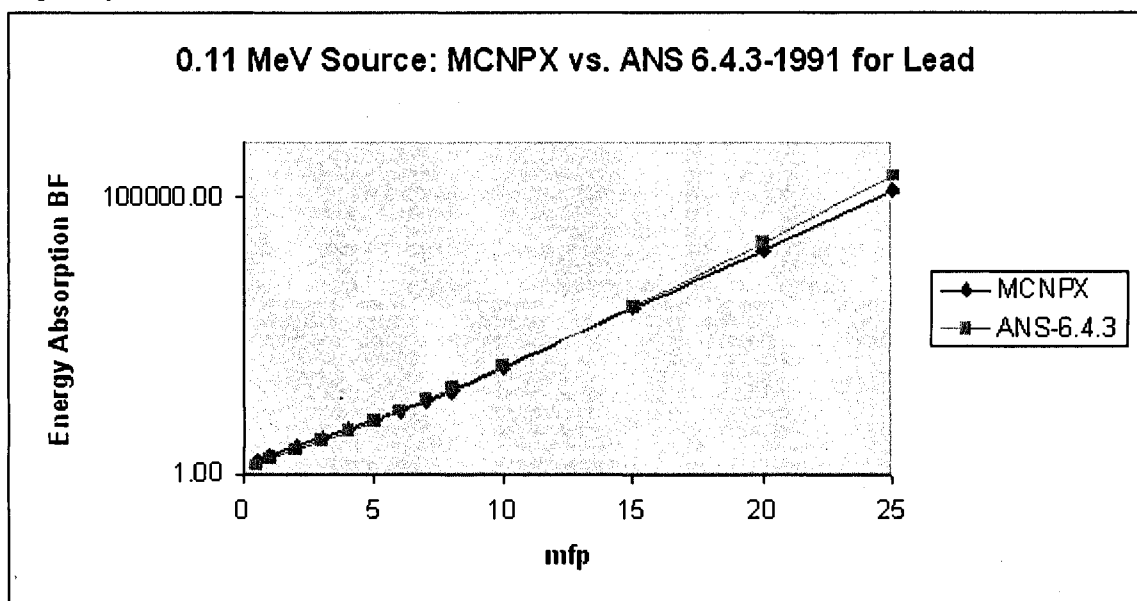


Table 6k MCNPX Energy Absorption Buildup Factor Compared to ANS-6.4.3-1991

Energy (MeV)	mfp (Lead)	Energy Absorption Buildup Factor New	Energy Absorption Buildup Factor ANS-6.4.3-1991	% Difference
0.120	0.500	1.71	1.46	17.28%
0.120	1.000	2.21	1.85	19.38%
0.120	2.000	3.10	2.62	18.16%
0.120	3.000	4.05	3.52	15.09%
0.120	4.000	5.24	4.71	11.26%
0.120	5.000	6.76	6.40	5.67%
0.120	6.000	8.82	8.77	0.56%
0.120	7.000	1.16E+01	1.23E+01	5.45%
0.120	8.000	1.58E+01	1.72E+01	8.39%
0.120	10.000	3.03E+01	3.39E+01	10.68%
0.120	15.000	2.01E+02	2.34E+02	14.15%
0.120	20.000	1.82E+03	2.06E+03	11.41%
0.120	25.000	1.64E+04	2.01E+04	18.21%
0.120	30.000	1.09E+05	2.04E+05	46.42%
0.120	35.000	*NO VALUE	2.10E+06	
0.120	40.000	*NO VALUE	2.18E+07	

\* The relative error in MCNPX was very high and Uncollided Dose was equal to zero

Figure 6k

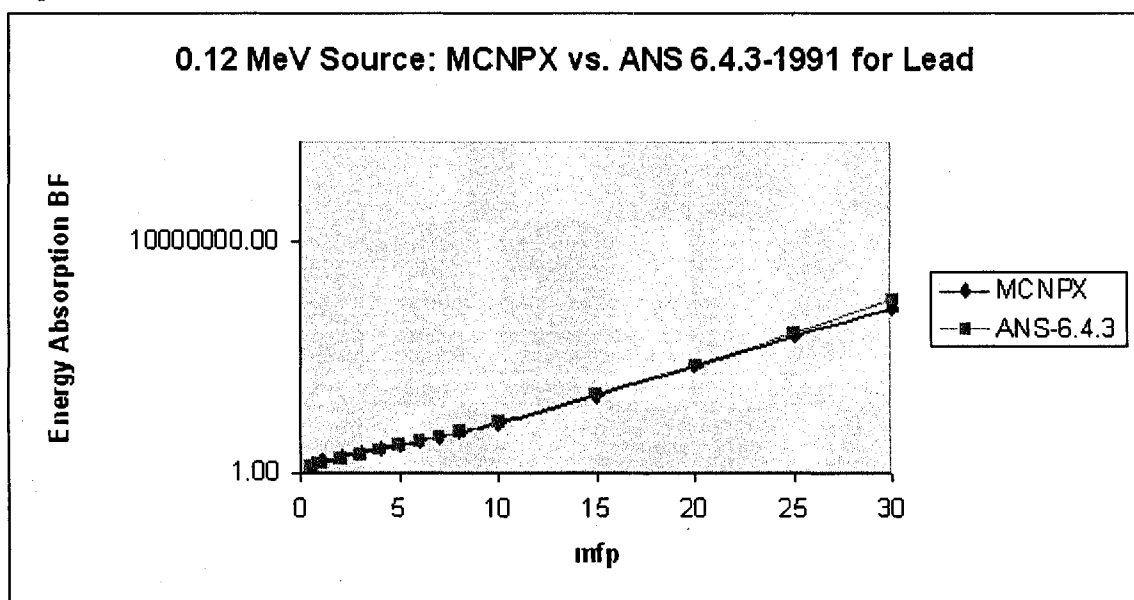




Table 6I MCNPX Energy Absorption Buildup Factor Compared to ANS-6.4.3-1991

Energy (MeV)	mfp (Lead)	Energy Absorption Buildup Factor New	Energy Absorption Buildup Factor ANS-6.4.3-1991	% Difference
0.13	0.500	1.70	1.46	16.26%
0.13	1.000	2.13	1.81	17.58%
0.13	2.000	2.80	2.41	16.11%
0.13	3.000	3.39	2.96	14.48%
0.13	4.000	3.97	3.59	10.68%
0.13	5.000	4.63	4.33	7.02%
0.13	6.000	5.39	5.23	3.08%
0.13	7.000	6.37	6.41	0.68%
0.13	8.000	7.57	7.98	5.10%
0.13	10.000	1.12E+01	1.22E+01	7.94%
0.13	15.000	4.05E+01	4.57E+01	11.39%
0.13	20.000	1.96E+02	2.20E+02	10.98%
0.13	25.000	1.10E+03	1.19E+03	7.32%
0.13	30.000	6.03E+03	6.68E+03	9.79%
0.13	35.000	2.31E+04	3.85E+04	40.00%
0.13	40.000	1.30E+05	2.25E+05	42.12%

Figure 6I

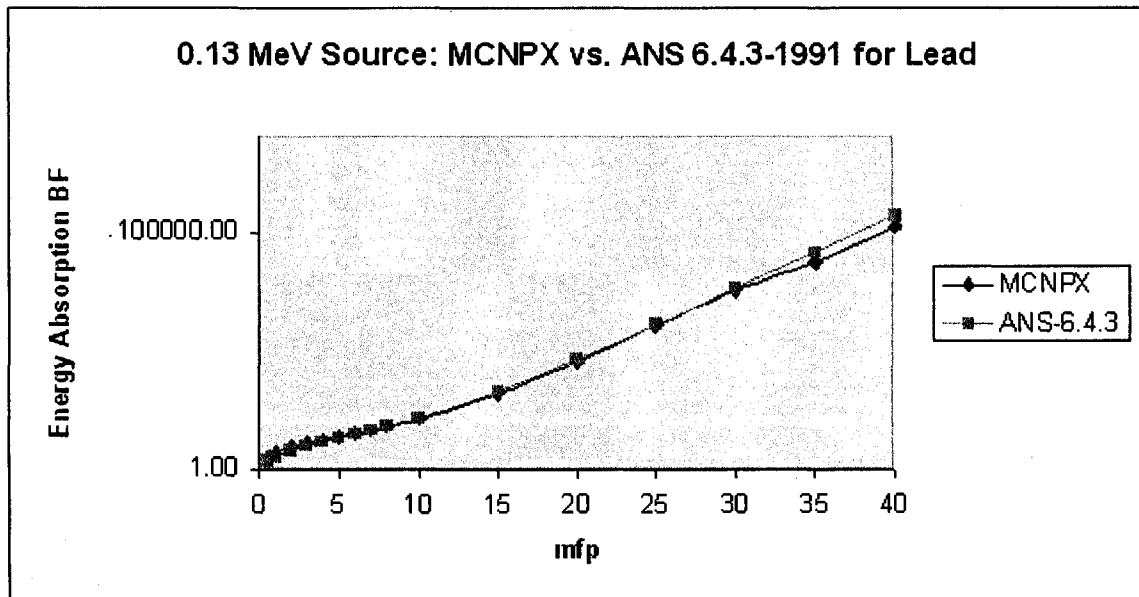


Table 6m MCNPX Energy Absorption Buildup Factor Compared to ANS-6.4.3-1991

Energy (MeV)	mfp (Lead)	Energy Absorption Buildup Factor New	Energy Absorption Buildup Factor ANS-6.4.3-1991	% Difference
0.14	0.500	1.68	1.45	15.74%
0.14	1.000	2.04	1.77	15.33%
0.14	2.000	2.53	2.20	14.84%
0.14	3.000	2.85	2.52	13.09%
0.14	4.000	3.12	2.81	11.12%
0.14	5.000	3.37	3.10	8.65%
0.14	6.000	3.64	3.39	7.29%
0.14	7.000	3.88	3.72	4.42%
0.14	8.000	4.22	4.11	2.63%
0.14	10.000	4.98	5.14	3.14%
0.14	15.000	8.91	9.52	6.37%
0.14	20.000	1.97E+01	2.17E+01	9.21%
0.14	25.000	5.10E+01	5.66E+01	9.97%
0.14	30.000	1.43E+02	1.60E+02	10.54%
0.14	35.000	4.24E+02	4.73E+02	10.41%
0.14	40.000	1.29E+03	1.44E+03	10.39%

Figure 6m

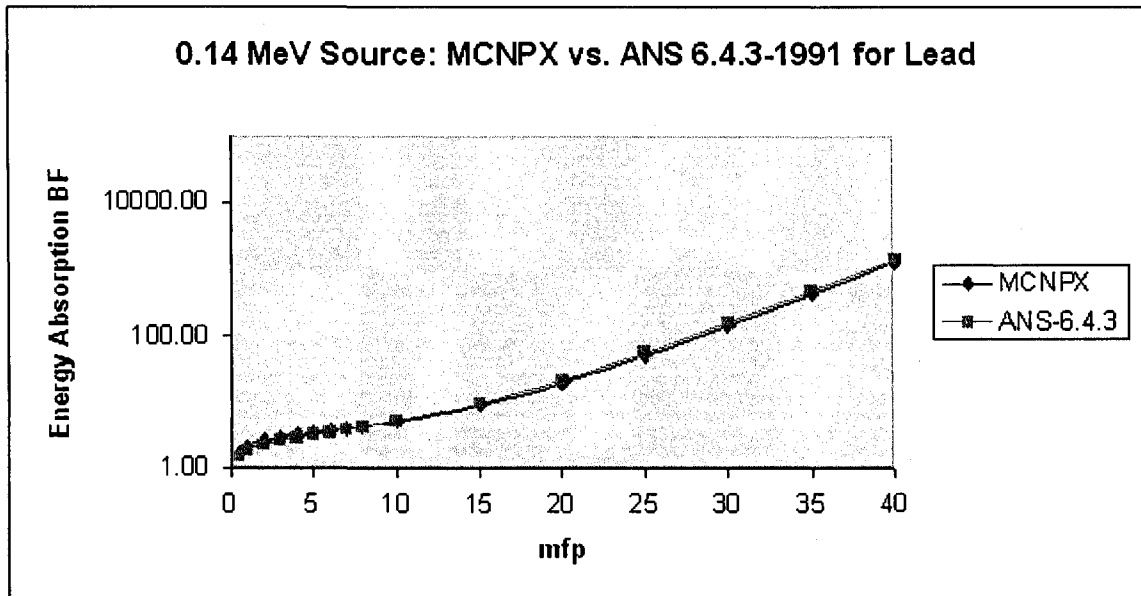


Table 6n MCNPX Energy Absorption Buildup Factor Compared to ANS-6.4.3-1991

Energy (MeV)	mfp (Lead)	Energy Absorption Buildup Factor New	Energy Absorption Buildup Factor ANS-6.4.3-1991	% Difference
0.15	0.500	1.65	1.45	13.50%
0.15	1.000	1.97	1.72	14.28%
0.15	2.000	2.30	2.03	13.22%
0.15	3.000	2.47	2.20	12.28%
0.15	4.000	2.58	2.32	11.20%
0.15	5.000	2.65	2.42	9.39%
0.15	6.000	2.71	2.49	8.67%
0.15	7.000	2.76	2.56	7.76%
0.15	8.000	2.81	2.64	6.47%
0.15	10.000	2.92	2.80	4.23%
0.15	15.000	3.25	3.28	0.85%
0.15	20.000	3.67	3.85	4.77%
0.15	25.000	4.25	4.50	5.55%
0.15	30.000	5.06	5.45	7.17%
0.15	35.000	6.30	6.89	8.60%
0.15	40.000	8.05	9.10	11.55%

Figure 6n

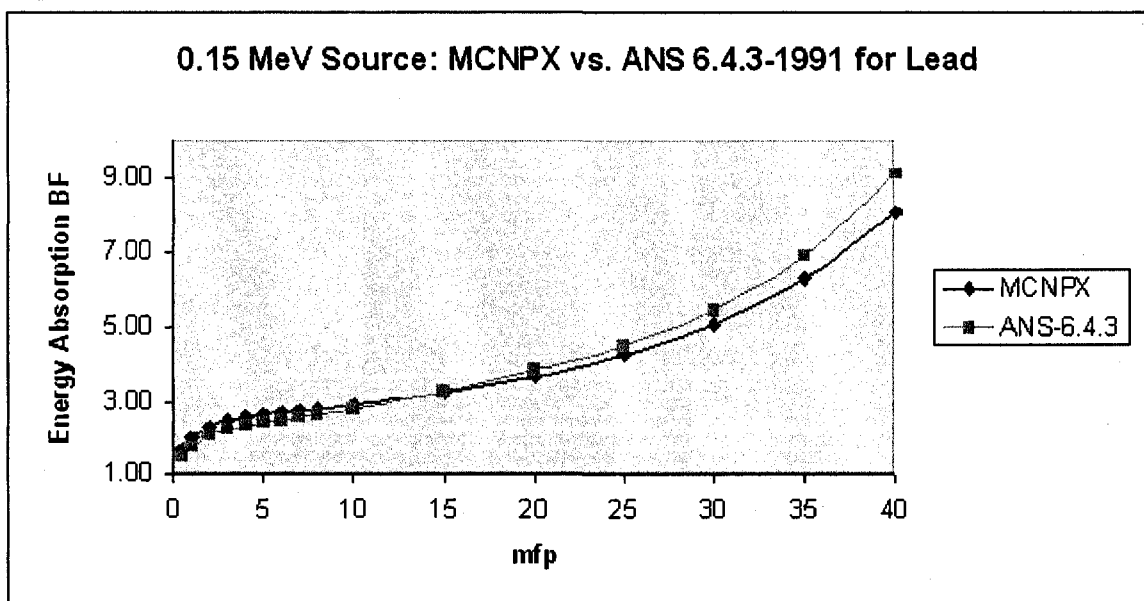


Table 6o MCNPX Energy Absorption Buildup Factor Compared to ANS-6.4.3-1991

Energy (MeV)	mfp (Lead)	Energy Absorption Buildup Factor New	Energy Absorption Buildup Factor ANS-6.4.3-1991	% Difference
0.16	0.500	1.65	1.45	13.66%
0.16	1.000	1.91	1.69	13.12%
0.16	2.000	2.14	1.91	12.21%
0.16	3.000	2.21	2.00	10.53%
0.16	4.000	2.25	2.05	9.63%
0.16	5.000	2.25	2.08	8.37%
0.16	6.000	2.26	2.09	8.22%
0.16	7.000	2.26	2.10	7.57%
0.16	8.000	2.27	2.11	7.57%
0.16	10.000	2.26	2.13	6.32%
0.16	15.000	2.25	2.15	4.85%
0.16	20.000	2.25	2.16	4.27%
0.16	25.000	2.24	2.16	3.75%
0.16	30.000	2.23	2.17	2.92%
0.16	35.000	2.23	2.17	2.99%
0.16	40.000	2.24	2.18	2.62%

Figure 6o

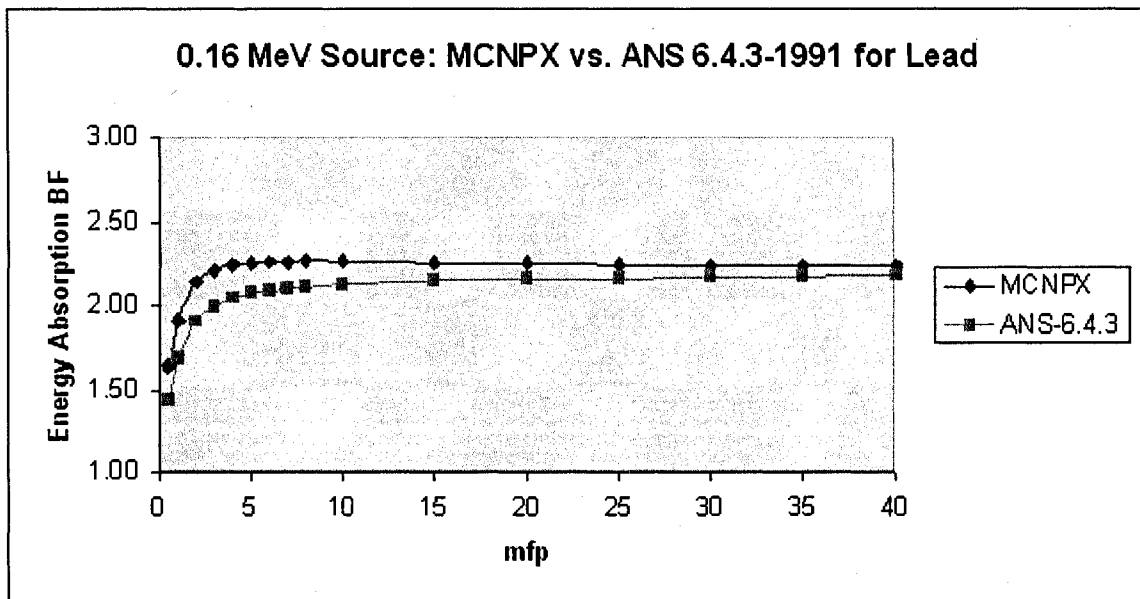


Table 6p MCNPX Energy Absorption Buildup Factor Compared to ANS-6.4.3-1991

Energy (MeV)	mfp (Lead)	Energy Absorption Buildup Factor New	Energy Absorption Buildup Factor ANS-6.4.3-1991	% Difference
0.20	0.500	1.60	1.47	8.69%
0.20	1.000	1.72	1.60	7.66%
0.20	2.000	1.76	1.66	6.13%
0.20	3.000	1.76	1.68	4.93%
0.20	4.000	1.78	1.69	5.27%
0.20	5.000	1.79	1.70	5.28%
0.20	6.000	1.80	1.72	4.61%
0.20	7.000	1.81	1.73	4.52%
0.20	8.000	1.82	1.75	3.91%
0.20	10.000	1.83	1.77	3.25%
0.20	15.000	1.85	1.83	1.32%
0.20	20.000	1.89	1.87	0.84%
0.20	25.000	1.89	1.91	0.92%
0.20	30.000	1.91	1.94	1.57%
0.20	35.000	1.92	1.97	2.64%
0.20	40.000	1.93	1.99	3.13%

Figure 6p

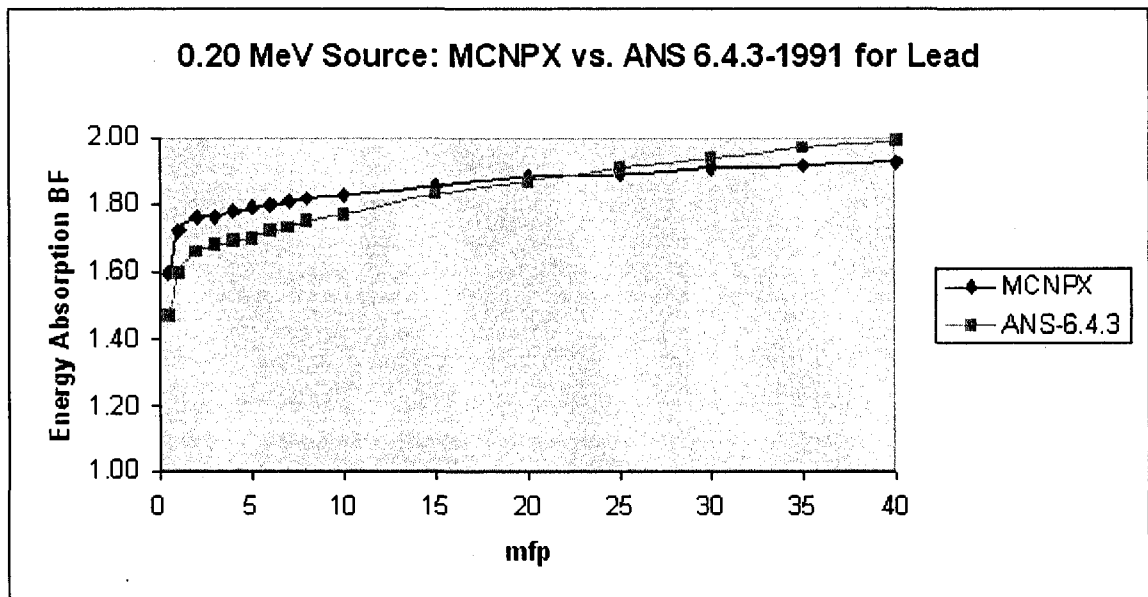


Table 6g MCNPX Energy Absorption Buildup Factor Compared to ANS-6.4.3-1991

Energy (MeV)	mfp (Lead)	Energy Absorption Buildup Factor New	Energy Absorption Buildup Factor ANS-6.4.3-1991	% Difference
0.30	0.500	1.50	1.43	5.07%
0.30	1.000	1.56	1.51	3.52%
0.30	2.000	1.65	1.61	2.28%
0.30	3.000	1.72	1.67	2.95%
0.30	4.000	1.78	1.72	3.55%
0.30	5.000	1.81	1.76	2.86%
0.30	6.000	1.85	1.80	2.89%
0.30	7.000	1.88	1.84	2.21%
0.30	8.000	1.90	1.87	1.72%
0.30	10.000	1.96	1.92	2.05%
0.30	15.000	2.04	2.03	0.30%
0.30	20.000	2.10	2.12	0.79%
0.30	25.000	2.13	2.19	2.62%
0.30	30.000	2.20	2.25	2.20%
0.30	35.000	2.22	2.30	3.42%
0.30	40.000	2.26	2.35	3.91%

Figure 6g

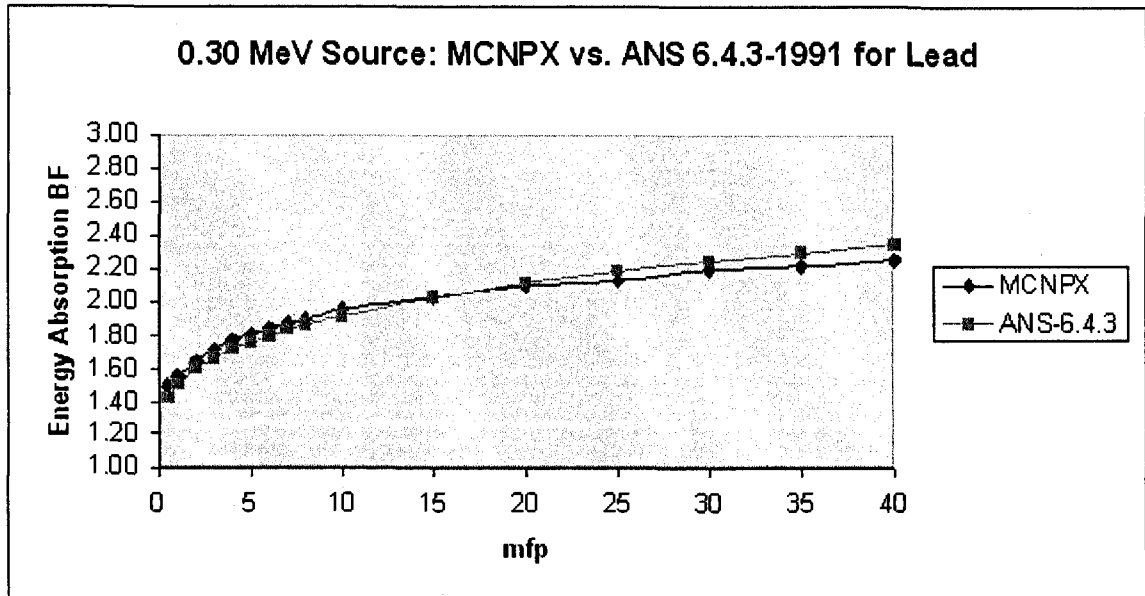


Table 6r MCNPX Energy Absorption Buildup Factor Compared to ANS-6.4.3-1991

Energy (MeV)	mfp (Lead)	Energy Absorption Buildup Factor New	Energy Absorption Buildup Factor ANS-6.4.3-1991	% Difference
0.40	0.500	1.49	1.45	2.47%
0.40	1.000	1.61	1.58	1.78%
0.40	2.000	1.78	1.76	1.23%
0.40	3.000	1.89	1.88	0.58%
0.40	4.000	1.99	1.98	0.55%
0.40	5.000	2.07	2.06	0.40%
0.40	6.000	2.15	2.15	0.04%
0.40	7.000	2.21	2.22	0.37%
0.40	8.000	2.27	2.28	0.54%
0.40	10.000	2.37	2.41	1.59%
0.40	15.000	2.55	2.66	3.99%
0.40	20.000	2.69	2.87	6.25%
0.40	25.000	2.78	3.04	8.60%
0.40	30.000	2.89	3.18	9.00%
0.40	35.000	2.97	3.30	10.00%
0.40	40.000	3.03	3.41	11.20%

Figure 6r

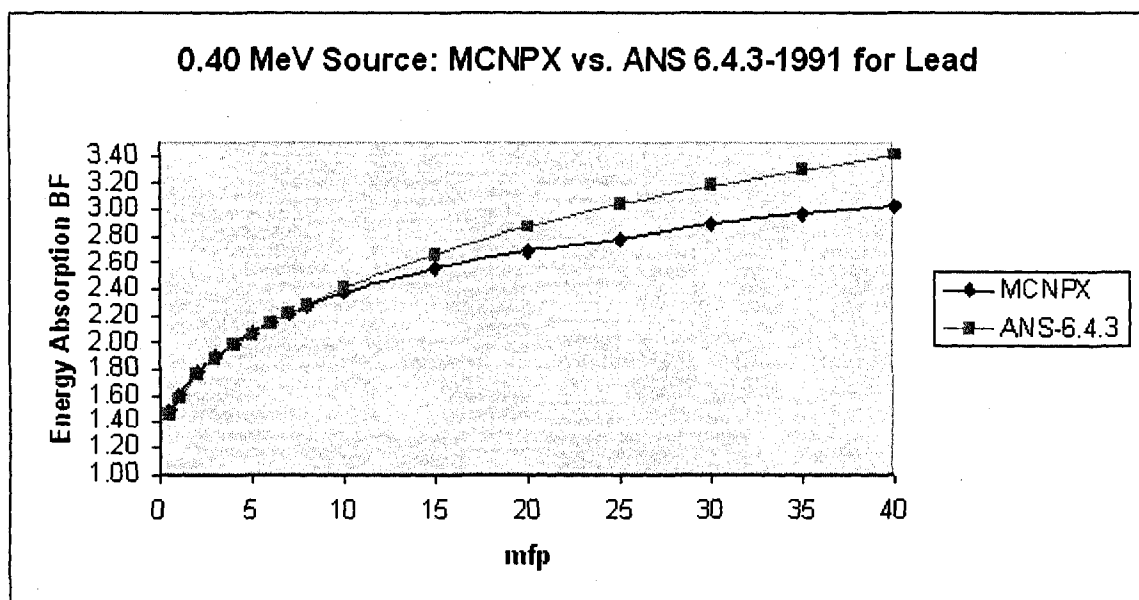


Table 6s MCNPX Energy Absorption Buildup Factor Compared to ANS-6.4.3-1991

Energy (MeV)	mfp (Lead)	Energy Absorption Buildup Factor New	Energy Absorption Buildup Factor ANS-6.4.3-1991	% Difference
0.50	0.500	1.52	1.48	2.74%
0.50	1.000	1.68	1.67	0.67%
0.50	2.000	1.93	1.92	0.61%
0.50	3.000	2.12	2.11	0.39%
0.50	4.000	2.28	2.26	0.91%
0.50	5.000	2.40	2.40	0.02%
0.50	6.000	2.53	2.53	0.11%
0.50	7.000	2.62	2.65	1.03%
0.50	8.000	2.72	2.76	1.62%
0.50	10.000	2.89	2.97	2.70%
0.50	15.000	3.22	3.41	5.62%
0.50	20.000	3.48	3.77	7.62%
0.50	25.000	3.66	4.07	9.99%
0.50	30.000	3.86	4.33	10.81%
0.50	35.000	4.04	4.56	11.45%
0.50	40.000	4.17	4.76	12.46%

Figure 6s

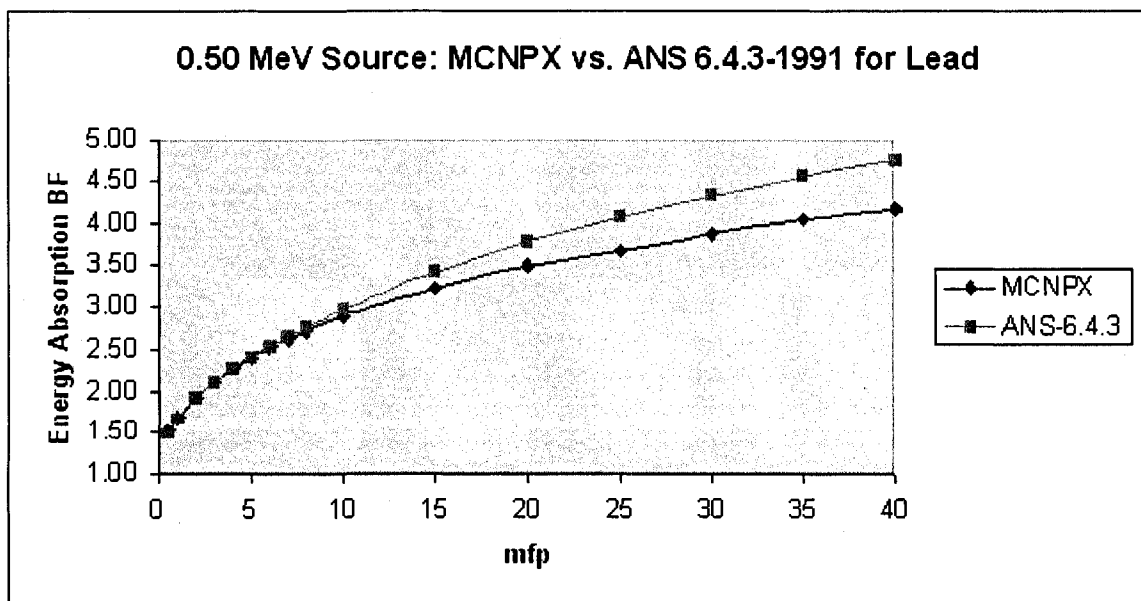




Table 6t MCNPX Energy Absorption Buildup Factor Compared to ANS-6.4.3-1991

Energy (MeV)	mfp (Lead)	Energy Absorption Buildup Factor New	Energy Absorption Buildup Factor ANS-6.4.3-1991	% Difference
0.60	0.500	1.54	1.36	13.43%
0.60	1.000	1.74	1.56	11.71%
0.60	2.000	2.06	1.85	11.58%
0.60	3.000	2.32	2.07	11.98%
0.60	4.000	2.54	2.25	13.04%
0.60	5.000	2.73	2.41	13.18%
0.60	6.000	2.90	2.58	12.35%
0.60	7.000	3.06	2.72	12.50%
0.60	8.000	3.19	2.85	11.85%
0.60	10.000	3.45	3.11	10.93%
0.60	15.000	3.95	3.65	8.13%
0.60	20.000	4.38	4.08	7.24%
0.60	25.000	4.72	4.44	6.38%
0.60	30.000	5.06	4.75	6.44%
0.60	35.000	5.31	5.03	5.61%
0.60	40.000	5.51	5.28	4.29%

Figure 6t

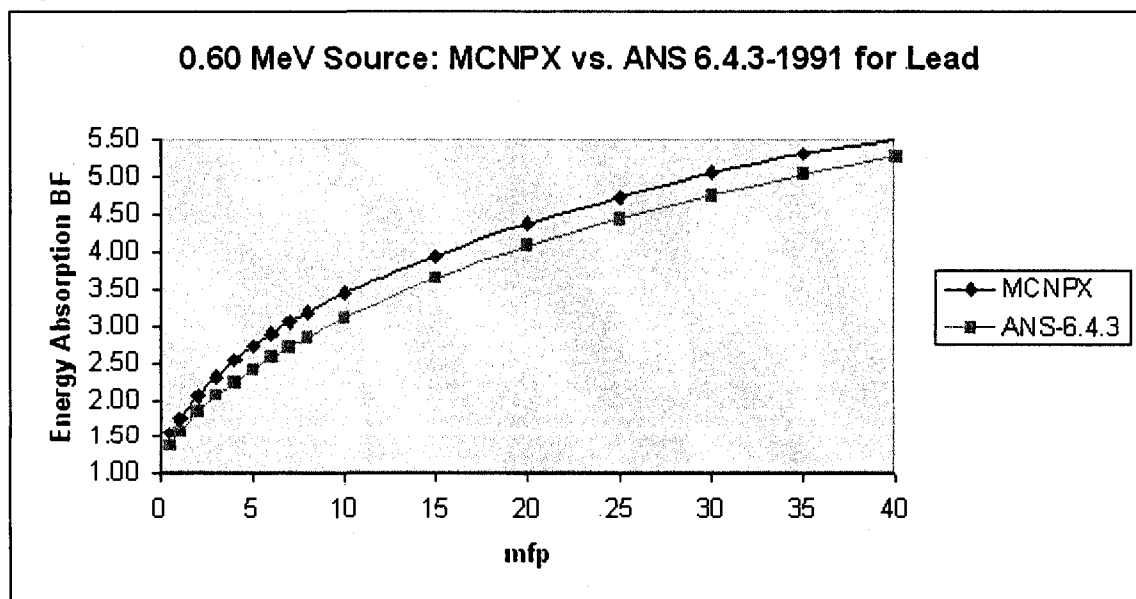


Table 6u MCNPX Energy Absorption Buildup Factor Compared to ANS-6.4.3-1991

Energy (MeV)	mfp (Lead)	Energy Absorption Buildup Factor New	Energy Absorption Buildup Factor ANS-6.4.3-1991	% Difference
0.80	0.500	1.58	1.43	10.46%
0.80	1.000	1.85	1.70	8.78%
0.80	2.000	2.29	2.09	9.49%
0.80	3.000	2.67	2.43	9.78%
0.80	4.000	2.99	2.70	10.66%
0.80	5.000	3.29	2.95	11.48%
0.80	6.000	3.57	3.22	10.77%
0.80	7.000	3.88	3.45	12.32%
0.80	8.000	4.07	3.67	10.82%
0.80	10.000	4.49	4.10	9.56%
0.80	15.000	5.45	5.03	8.34%
0.80	20.000	6.29	5.82	8.13%
0.80	25.000	6.97	6.49	7.34%
0.80	30.000	7.57	7.09	6.73%
0.80	35.000	8.16	7.64	6.86%
0.80	40.000	8.65	8.13	6.44%

Figure 6u

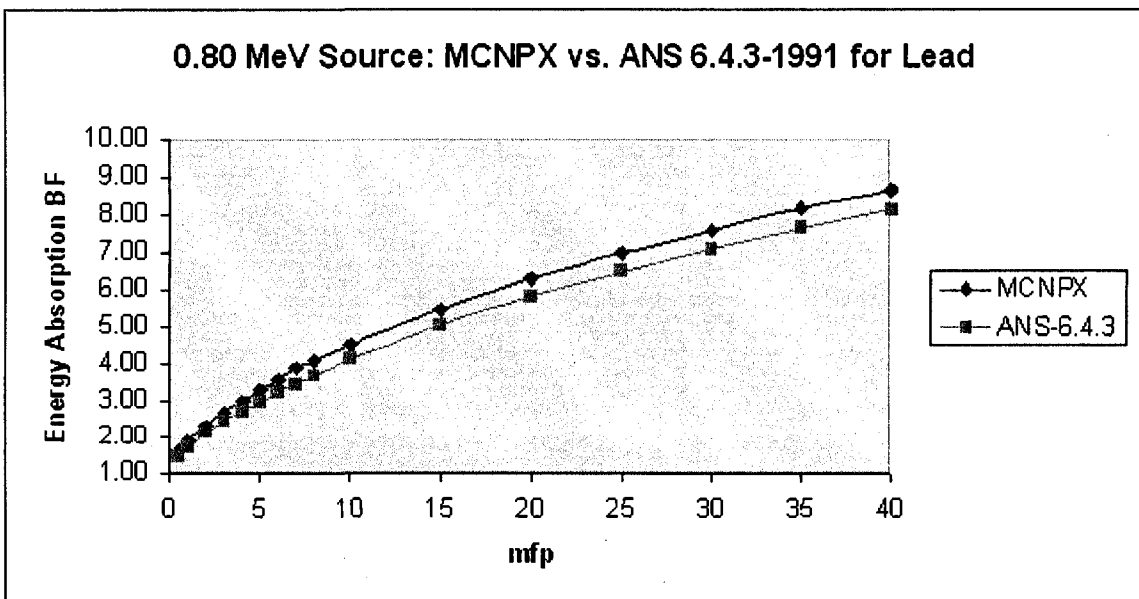


Table 6v MCNPX Energy Absorption Buildup Factor Compared to ANS-6.4.3-1991

Energy (MeV)	mfp (Lead)	Energy Absorption Buildup Factor New	Energy Absorption Buildup Factor ANS-6.4.3-1991	% Difference
1.00	0.500	1.59	1.46	8.91%
1.00	1.000	1.90	1.76	7.77%
1.00	2.000	2.42	2.23	8.50%
1.00	3.000	2.89	2.64	9.30%
1.00	4.000	3.29	2.99	10.19%
1.00	5.000	3.68	3.32	10.94%
1.00	6.000	4.04	3.68	9.66%
1.00	7.000	4.37	4.00	9.14%
1.00	8.000	4.72	4.30	9.80%
1.00	10.000	5.31	4.90	8.35%
1.00	15.000	6.70	6.26	7.10%
1.00	20.000	8.00	7.44	7.54%
1.00	25.000	8.99	8.48	6.03%
1.00	30.000	1.00E+01	9.41	6.48%
1.00	35.000	1.09E+01	1.03E+01	6.10%
1.00	40.000	1.17E+01	1.11E+01	5.02%

Figure 6v

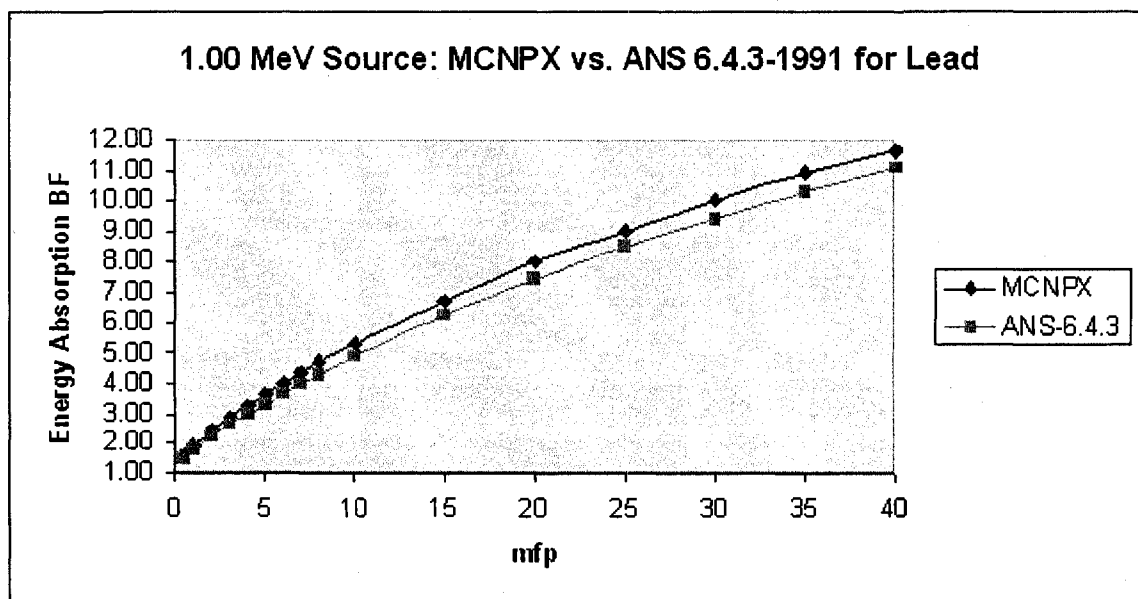


Table 6w MCNPX Energy Absorption Buildup Factor Compared to ANS-6.4.3-1991

Energy (MeV)	mfp (Lead)	Energy Absorption Buildup Factor New	Energy Absorption Buildup Factor ANS-6.4.3-1991	% Difference
1.50	0.500	1.61	1.43	12.74%
1.50	1.000	1.96	1.75	12.01%
1.00	2.000	2.57	2.29	12.02%
1.00	3.000	3.14	2.82	11.21%
1.00	4.000	3.70	3.31	11.76%
1.00	5.000	4.24	3.81	11.21%
1.00	6.000	4.75	4.34	9.43%
1.00	7.000	5.29	4.85	9.07%
1.00	8.000	5.80	5.36	8.15%
1.00	10.000	6.82	6.40	6.58%
1.00	15.000	9.30	9.08	2.42%
1.00	20.000	1.18E+01	1.18E+01	0.26%
1.00	25.000	1.43E+01	1.46E+01	2.03%
1.00	30.000	1.68E+01	1.72E+01	2.09%
1.00	35.000	1.94E+01	1.97E+01	1.48%
1.00	40.000	2.18E+01	2.22E+01	1.89%

Figure 6w

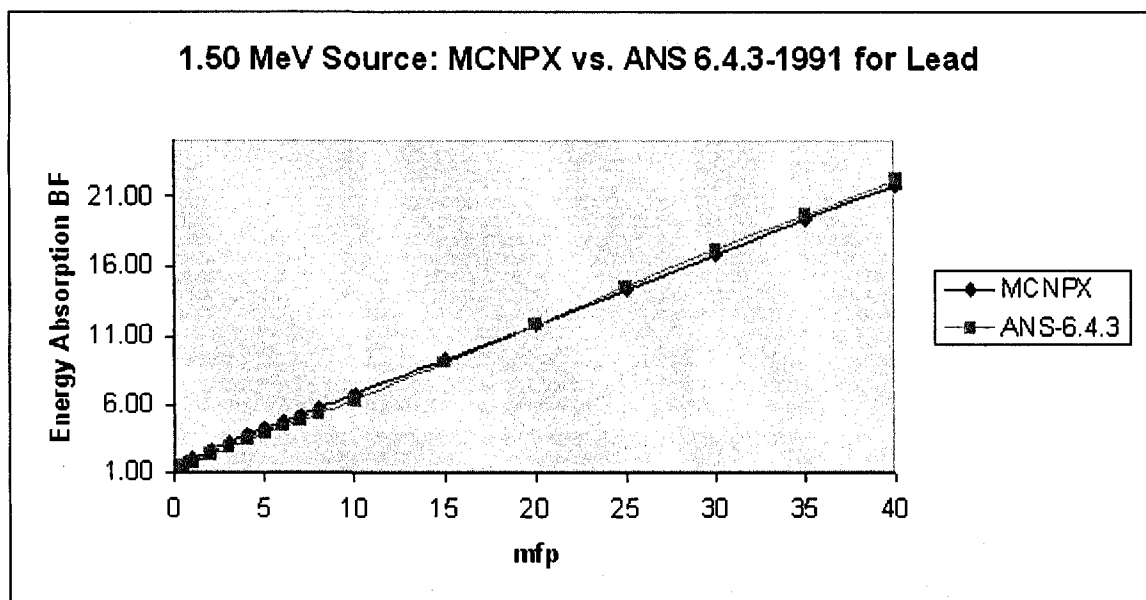


Table 6x MCNPX Energy Absorption Buildup Factor Compared to ANS-6.4.3-1991

Energy (MeV)	mfp (Lead)	Energy Absorption Buildup Factor New	Energy Absorption Buildup Factor ANS-6.4.3-1991	% Difference
2.00	0.500	1.62	1.48	9.61%
2.00	1.000	1.95	1.78	9.64%
2.00	2.000	2.54	2.28	11.52%
2.00	3.000	3.13	2.82	10.83%
2.00	4.000	3.72	3.35	11.15%
2.00	5.000	4.36	3.90	11.71%
2.00	6.000	4.97	4.50	10.39%
2.00	7.000	5.61	5.08	10.40%
2.00	8.000	6.26	5.68	10.13%
2.00	10.000	7.54	6.95	8.46%
2.00	15.000	1.11E+01	1.03E+01	8.03%
2.00	20.000	1.50E+01	1.39E+01	7.90%
2.00	25.000	1.91E+01	1.77E+01	7.93%
2.00	30.000	2.33E+01	2.15E+01	8.60%
2.00	35.000	2.77E+01	2.55E+01	8.51%
2.00	40.000	3.15E+01	2.94E+01	7.03%

Figure 6x

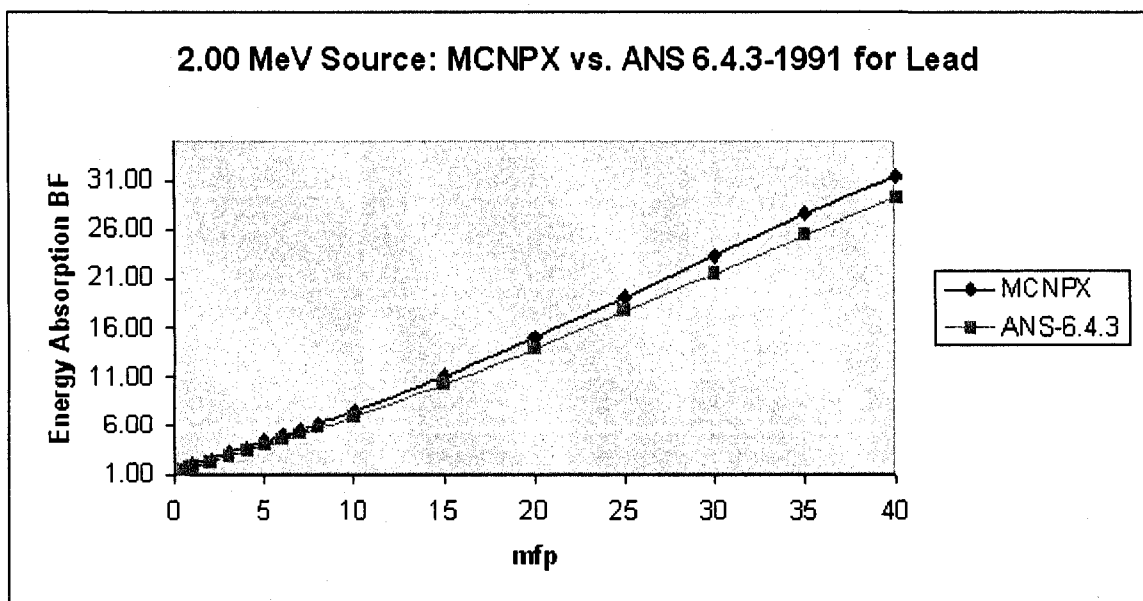


Table 6y MCNPX Energy Absorption Buildup Factor Compared to ANS-6.4.3-1991

Energy (MeV)	mfp (Lead)	Energy Absorption Buildup Factor New	Energy Absorption Buildup Factor ANS-6.4.3-1991	% Difference
3.00	0.500	1.57	1.49	5.33%
3.00	1.000	1.83	1.71	7.24%
3.00	2.000	2.32	2.11	9.72%
3.00	3.000	2.84	2.56	10.88%
3.00	4.000	3.39	3.03	12.04%
3.00	5.000	3.99	3.55	12.46%
3.00	6.000	4.60	4.12	11.73%
3.00	7.000	5.26	4.72	11.35%
3.00	8.000	5.97	5.34	11.78%
3.00	10.000	7.54	6.73	12.01%
3.00	15.000	1.22E+01	1.08E+01	13.25%
3.00	20.000	1.79E+01	1.57E+01	14.05%
3.00	25.000	2.40E+01	2.12E+01	13.39%
3.00	30.000	3.12E+01	2.74E+01	13.77%
3.00	35.000	4.01E+01	3.41E+01	17.62%
3.00	40.000	4.99E+01	4.14E+01	20.44%

Figure 6y

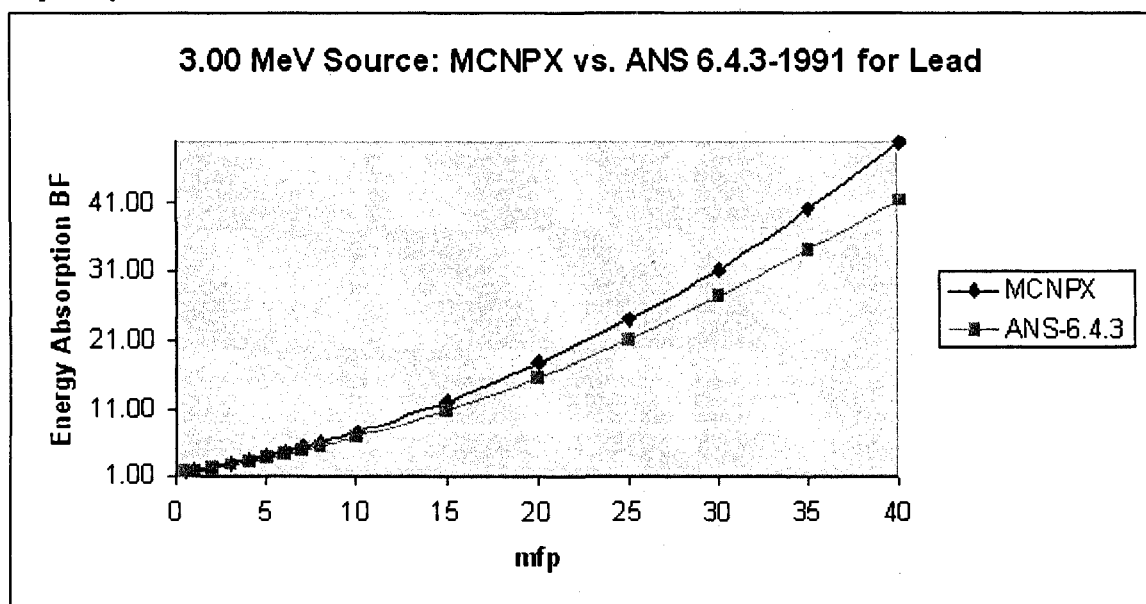


Table 6z MCNPX Energy Absorption Buildup Factor Compared to ANS-6.4.3-1991

Energy (MeV)	mfp (Lead)	Energy Absorption Buildup Factor New	Energy Absorption Buildup Factor ANS-6.4.3-1991	% Difference
4.00	0.500	1.51	1.43	5.55%
4.00	1.000	1.73	1.60	8.14%
4.00	2.000	2.13	1.91	11.73%
4.00	3.000	2.57	2.28	12.80%
4.00	4.000	3.04	2.68	13.61%
4.00	5.000	3.58	3.12	14.68%
4.00	6.000	4.19	3.61	15.97%
4.00	7.000	4.81	4.15	16.02%
4.00	8.000	5.50	4.73	16.33%
4.00	10.000	7.12	6.06	17.46%
4.00	15.000	1.22E+01	1.04E+01	17.11%
4.00	20.000	1.96E+01	1.64E+01	19.68%
4.00	25.000	2.90E+01	2.43E+01	19.40%
4.00	30.000	4.16E+01	3.44E+01	20.88%
4.00	35.000	6.06E+01	4.70E+01	28.88%
4.00	40.000	8.45E+01	6.24E+01	35.49%

Figure 6z

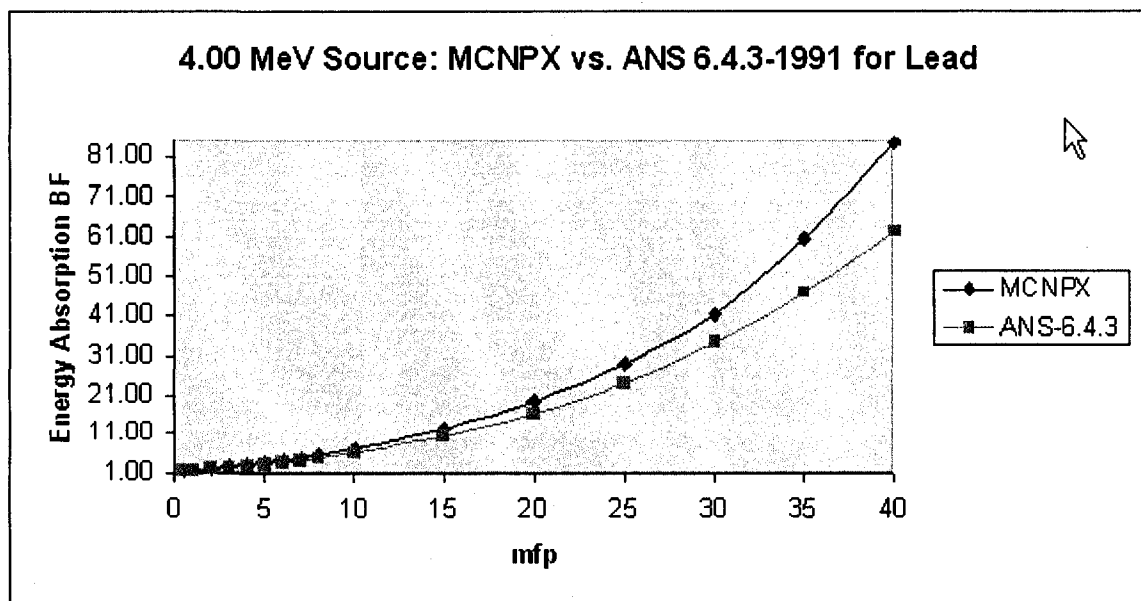


Table 6aa MCNPX Energy Absorption Buildup Factor Compared to ANS-6.4.3-1991

Energy (MeV)	mfp (Lead)	Energy Absorption Buildup Factor New	Energy Absorption Buildup Factor ANS-6.4.3-1991	% Difference
5.00	0.500	1.47	1.44	1.97%
5.00	1.000	1.66	1.62	2.69%
5.00	2.000	2.01	1.89	6.60%
5.00	3.000	2.40	2.22	8.32%
5.00	4.000	2.84	2.59	9.69%
5.00	5.000	3.34	3.00	11.25%
5.00	6.000	3.91	3.48	12.33%
5.00	7.000	4.55	4.02	13.08%
5.00	8.000	5.23	4.60	13.75%
5.00	10.000	6.79	6.01	12.95%
5.00	15.000	1.28E+01	1.11E+01	15.25%
5.00	20.000	2.19E+01	1.91E+01	14.82%
5.00	25.000	3.54E+01	3.13E+01	12.98%
5.00	30.000	5.64E+01	4.93E+01	14.48%
5.00	35.000	8.25E+01	7.51E+01	9.84%
5.00	40.000	1.17E+02	1.11E+02	5.38%

Figure 6aa

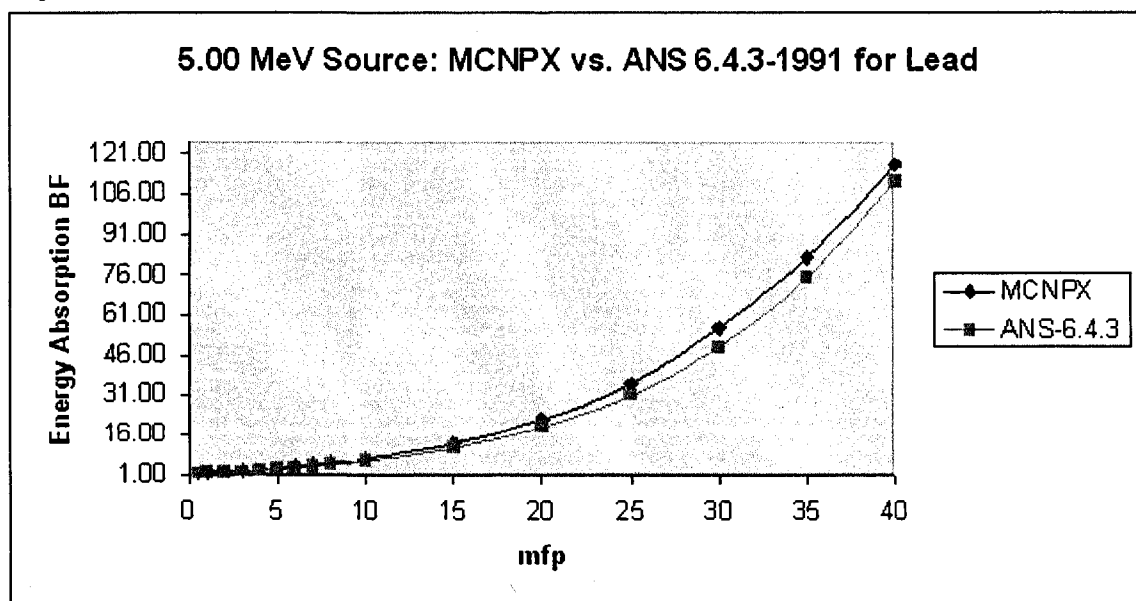




Table 6ab MCNPX Energy Absorption Buildup Factor Compared to ANS-6.4.3-1991

Energy (MeV)	mfp (Lead)	Energy Absorption Buildup Factor New	Energy Absorption Buildup Factor ANS-6.4.3-1991	% Difference
6.00	0.500	1.44	1.41	1.83%
6.00	1.000	1.62	1.58	2.38%
6.00	2.000	1.94	1.84	5.56%
6.00	3.000	2.33	2.15	8.39%
6.00	4.000	2.76	2.50	10.34%
6.00	5.000	3.27	2.91	12.41%
6.00	6.000	3.83	3.40	12.68%
6.00	7.000	4.49	3.94	13.89%
6.00	8.000	5.21	4.56	14.23%
6.00	10.000	7.03	6.08	15.59%
6.00	15.000	1.42E+01	1.21E+01	17.44%
6.00	20.000	2.68E+01	2.31E+01	16.02%
6.00	25.000	5.14E+01	4.26E+01	20.63%
6.00	30.000	8.87E+01	7.57E+01	17.22%
6.00	35.000	1.65E+02	1.31E+02	25.87%
6.00	40.000	2.86E+02	2.21E+02	29.63%

Figure 6ab

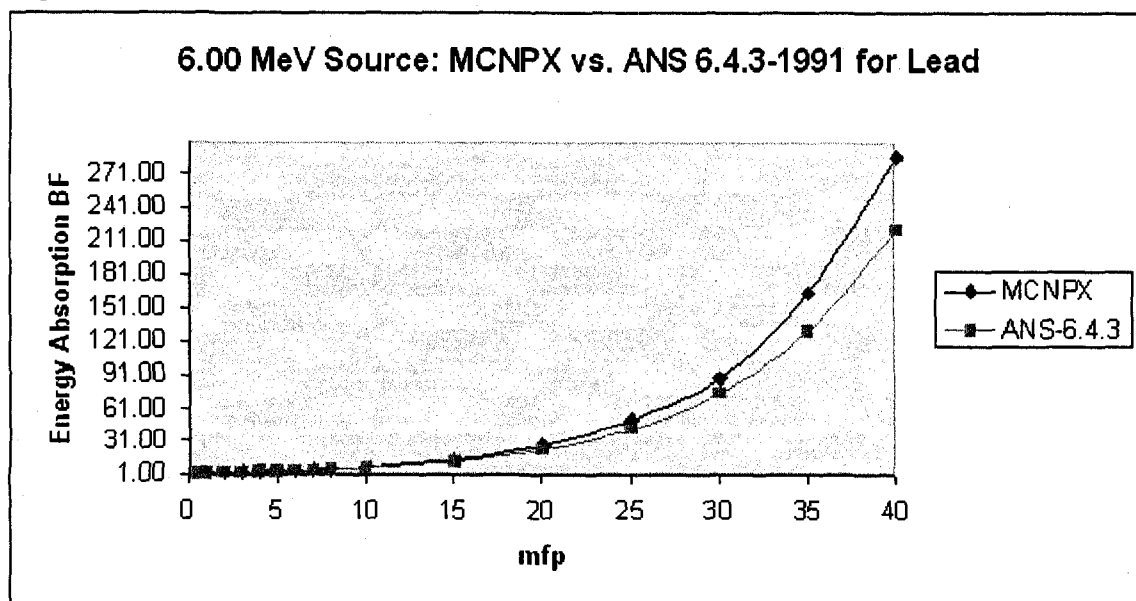


Table 6ac MCNPX Energy Absorption Buildup Factor Compared to ANS-6.4.3-1991

Energy (MeV)	mfp (Lead)	Energy Absorption Buildup Factor New	Energy Absorption Buildup Factor ANS-6.4.3-1991	% Difference
8.00	0.500	1.39	1.40	0.36%
8.00	1.000	1.57	1.59	1.09%
8.00	2.000	1.91	1.89	0.92%
8.00	3.000	2.29	2.24	2.09%
8.00	4.000	2.76	2.66	3.83%
8.00	5.000	3.33	3.17	5.14%
8.00	6.000	4.00	3.79	5.48%
8.00	7.000	4.82	4.53	6.33%
8.00	8.000	5.75	5.41	6.34%
8.00	10.000	8.17	7.76	5.23%
8.00	15.000	2.05E+01	1.90E+01	7.78%
8.00	20.000	5.03E+01	4.59E+01	9.67%
8.00	25.000	1.16E+02	1.08E+02	7.50%
8.00	30.000	2.57E+02	2.49E+02	3.19%
8.00	35.000	6.05E+02	5.62E+02	7.63%
8.00	40.000	9.63E+02	1.24E+03	22.35%

Figure 6ac

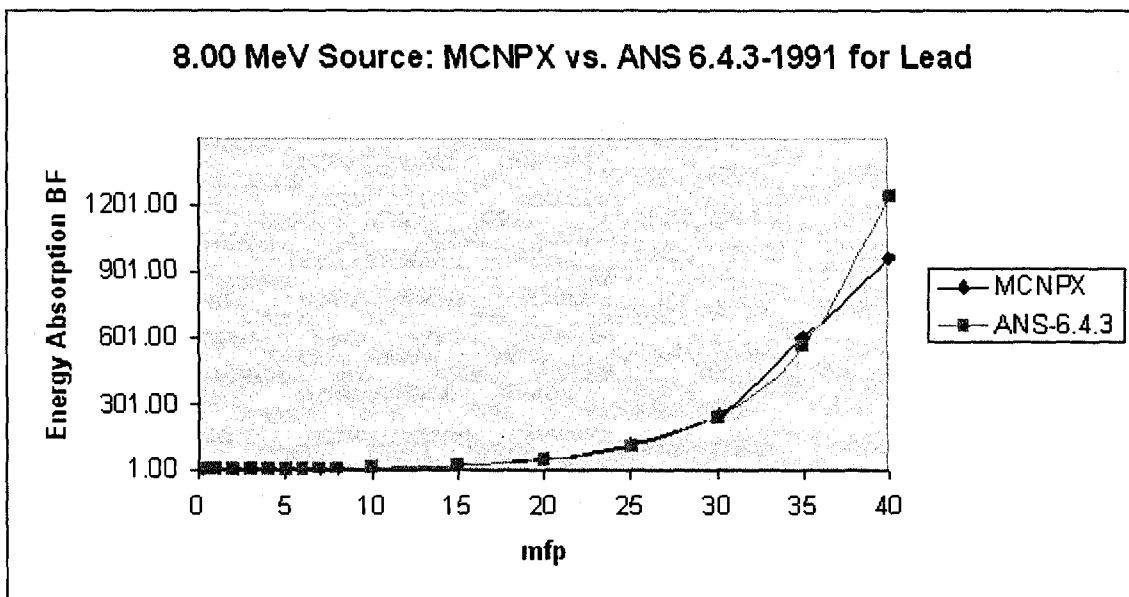


Table 6ad MCNPX Energy Absorption Buildup Factor Compared to ANS-6.4.3-1991

Energy (MeV)	mfp (Lead)	Energy Absorption Buildup Factor New	Energy Absorption Buildup Factor ANS-6.4.3-1991	% Difference
10.00	0.500	1.37	1.35	1.77%
10.00	1.000	1.56	1.54	1.39%
10.00	2.000	1.92	1.88	2.02%
10.00	3.000	2.36	2.30	2.56%
10.00	4.000	2.90	2.85	1.74%
10.00	5.000	3.60	3.54	1.81%
10.00	6.000	4.45	4.40	1.14%
10.00	7.000	5.54	5.50	0.67%
10.00	8.000	6.88	6.87	0.17%
10.00	10.000	1.07E+01	1.08E+01	1.12%
10.00	15.000	3.28E+01	3.38E+01	3.02%
10.00	20.000	1.02E+02	1.05E+02	2.90%
10.00	25.000	3.30E+02	3.19E+02	3.60%
10.00	30.000	9.71E+02	9.44E+02	2.89%
10.00	35.000	2.28E+03	2.73E+03	16.53%
10.00	40.000	1.19E+04	7.75E+03	53.65%

Figure 6ad

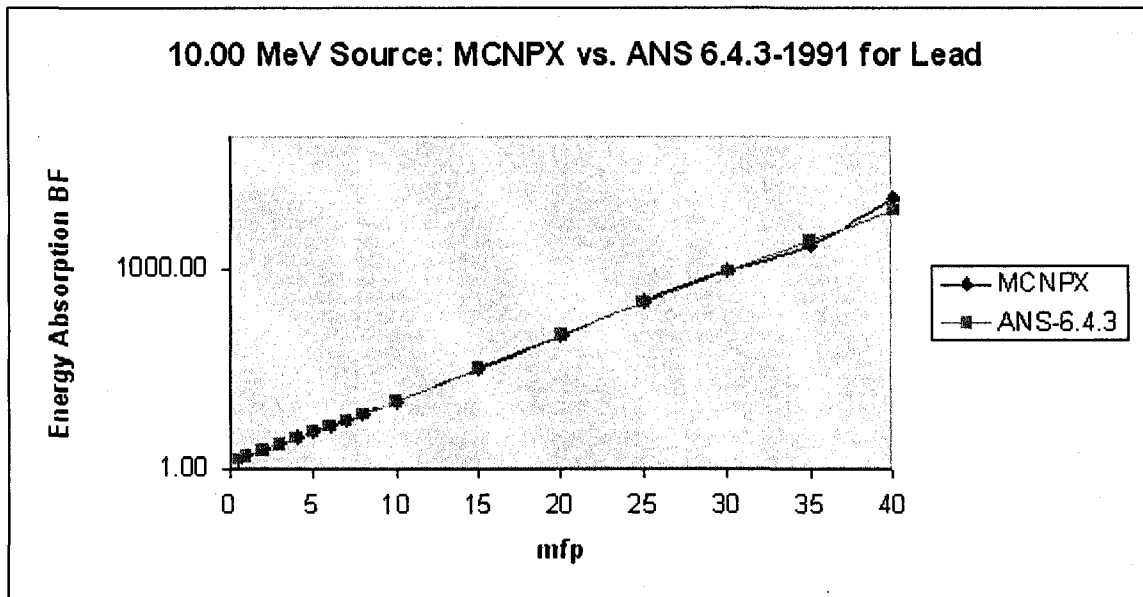
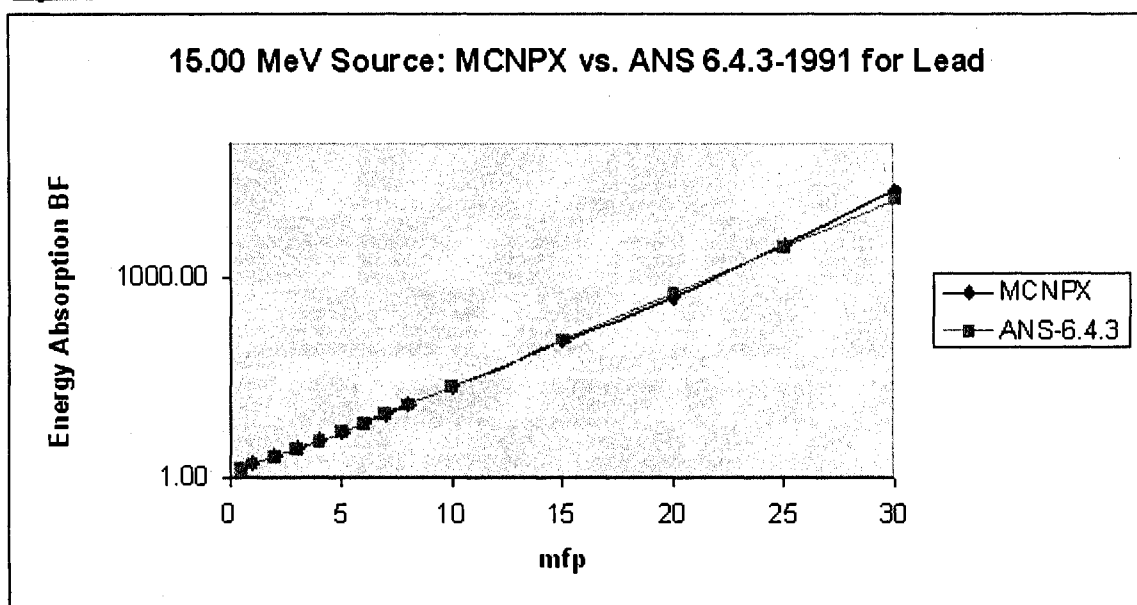


Table 6ae MCNPX Energy Absorption Buildup Factor Compared to ANS-6.4.3-1991

Energy (MeV)	mfp (Lead)	Energy Absorption Buildup Factor New	Energy Absorption Buildup Factor ANS-6.4.3-1991	% Difference
15.00	0.500	1.35	1.32	2.53%
15.00	1.000	1.58	1.55	1.66%
15.00	2.000	2.05	1.99	3.08%
15.00	3.000	2.69	2.58	4.20%
15.00	4.000	3.55	3.42	3.81%
15.00	5.000	4.74	4.61	2.76%
15.00	6.000	6.40	6.26	2.18%
15.00	7.000	8.80	8.56	2.82%
15.00	8.000	11.97	11.80	1.48%
15.00	10.000	2.23E+01	2.26E+01	1.27%
15.00	15.000	1.10E+02	1.17E+02	6.32%
15.00	20.000	5.03E+02	5.94E+02	15.24%
15.00	25.000	3.20E+03	2.93E+03	9.36%
15.00	30.000	1.96E+04	1.41E+04	38.78%
15.00	35.000	*NO VALUE	6.62E+04	
15.00	40.000	*NO VALUE	3.05E+05	

\* The relative error in MCNPX was very high and Uncollided Dose was equal to zero

Figure 6ae



## APPENDIX VII

### PALLAS-1D (VII) Sample Input File

```
60 38 44
# PB 15 MEV , POINT ISOTROPIC SOURCE PAL3.(PB15AA)
4 0 0 0
2 10 1 1 1
44
4 38 0 0
10 0 0 0
15.00 0.50 1.0 0.05
11 10 6 33
0.35225 1.2067 1.609 12.872
1 1 1 1
1 1 1 1
LEAD
820
11.34 0.088
0.03296 0.0
8 1 1 1 0 0
1 15 21 27 32 36 40 60
0.0310 0.5 1.0 2.0 3.0 4.0 5.0 10.0
```

## APPENDIX VIII

### MCNPX Sample Input File

```
C LEAD INFINITE MEDIUM 0.15 MEV UP TO 40 MFP
1 1 -11.34 -1 $INNER SPHERE 1: SOURCE CELL
2 1 -11.34 1 -2 $$SHELL 2
3 1 -11.34 2 -3 $$SHELL 3
4 1 -11.34 3 -4 $$SHELL 4
5 1 -11.34 4 -5 $$SHELL 5
6 1 -11.34 5 -6 $$SHELL 6
7 1 -11.34 6 -7 $$SHELL 7
8 1 -11.34 7 -8 $$SHELL 8
9 1 -11.34 8 -9 $$SHELL 9
10 1 -11.34 9 -10 $$SHELL 10
11 1 -11.34 10 -11 $$SHELL 11
12 1 -11.34 11 -12 $$SHELL 12
13 1 -11.34 12 -13 $$SHELL 13
14 1 -11.34 13 -14 $$SHELL 14
15 1 -11.34 14 -15 $$SHELL 15
16 1 -11.34 15 -16 $$SHELL 16
17 1 -11.34 16 -17 $$SHELL 17
18 1 -11.34 17 -18 $$SHELL 18
19 1 -11.34 18 -19 $$SHELL 19
20 1 -11.34 19 -20 $$SHELL 20
21 1 -11.34 20 -21 $$SHELL 21
22 1 -11.34 21 -22 $$SHELL 22
23 1 -11.34 22 -23 $$SHELL 23
24 1 -11.34 23 -24 $$SHELL 24
25 1 -11.34 24 -25 $$SHELL 25
26 1 -11.34 25 -26 $$SHELL 26
27 1 -11.34 26 -27 $$SHELL 27
28 1 -11.34 27 -28 $$SHELL 28
29 1 -11.34 28 -29 $$SHELL 29
30 1 -11.34 29 -30 $$SHELL 30
31 1 -11.34 30 -31 $$SHELL 31
32 1 -11.34 31 -32 $$SHELL 32
33 1 -11.34 32 -33 $$SHELL 33
34 1 -11.34 33 -34 $$SHELL 34
35 1 -11.34 34 -35 $$SHELL 35
36 1 -11.34 35 -36 $$SHELL 36
37 1 -11.34 36 -37 $$SHELL 37
38 1 -11.34 37 -38 $$SHELL 38
39 1 -11.34 38 -39 $$SHELL 39
40 1 -11.34 39 -40 $$SHELL 40
41 1 -11.34 40 -41 $$SHELL 41
42 0 41 -42 $OUTSIDE OF MATERIAL BUT WITHIN LIMIT OF SPACE
43 0 42 $OUTSIDE SPACE LIMIT
```

C ALL MFP @ 0.15MEV IN PB  
 1 SO 0.021956 \$0.5 MFP  
 2 SO 0.043912 \$1 MFP  
 3 SO 0.087823 \$2MFP  
 4 SO 0.13173 \$3 MFP  
 5 SO 0.17565 \$4 MFP  
 6 SO 0.21956 \$5 MFP  
 7 SO 0.26347 \$6 MFP  
 8 SO 0.30738 \$7 MFP  
 9 SO 0.35129 \$8 MFP  
 10 SO 0.395200 \$CELL ADDITION  
 11 SO 0.43912 \$10 MFP  
 12 SO 0.475700 \$CELL ADDITION  
 13 SO 0.512300 \$CELL ADDITION  
 14 SO 0.548900 \$CELL ADDITION  
 15 SO 0.585500 \$CELL ADDITION  
 16 SO 0.622100 \$CELL ADDITION  
 17 SO 0.65867 \$15 MFP  
 18 SO 0.695300 \$CELL ADDITION  
 19 SO 0.731900 \$CELL ADDITION  
 20 SO 0.768500 \$CELL ADDITION  
 21 SO 0.805000 \$CELL ADDITION  
 22 SO 0.841600 \$CELL ADDITION  
 23 SO 0.87823 \$20 MFP  
 24 SO 0.922100 \$CELL ADDITION  
 25 SO 0.966100 \$CELL ADDITION  
 26 SO 1.01000 \$CELL ADDITION  
 27 SO 1.05400 \$CELL ADDITION  
 28 SO 1.0978 \$25 MFP  
 29 SO 1.15300 \$CELL ADDITION  
 30 SO 1.20800 \$CELL ADDITION  
 31 SO 1.26200 \$CELL ADDITION  
 32 SO 1.3173 \$30 MFP  
 33 SO 1.37200 \$CELL ADDITION  
 34 SO 1.42700 \$CELL ADDITION  
 35 SO 1.48200 \$CELL ADDITION  
 36 SO 1.5369 \$35 MFP  
 37 SO 1.59200 \$CELL ADDITION  
 38 SO 1.64700 \$CELL ADDITION  
 39 SO 1.70200 \$CELL ADDITION  
 40 SO 1.7565 \$40 MFP  
 41 SO 3.0 \$3CM OF LEAD  
 42 SO 4.0 \$LIMIT OF SPACE

# MODE P

IMP:P 10 15 18 40 97 244 619 1576 4029 10271 26250 66775  
 145577 318150 694715 1516718 3312169 7218410 15746795  
 34323068 74850011 162675387 354041396 774480755  
 1967938990 5011705808 12687990047 32194568706 81647595140  
 262166775066 836146931211 2609188925750 8338987191255  
 26337906834259 83335799613621 263484942557841  
 829768753836972 2620043484444200 8214169962537140  
 25719394832372500 80320316337438800 0 0

C  
 M1 82000.04P 1.  
 C M1 82000 1.

```

C
SDEF POS 0 0 0 ERG 0.15
C
FC2 DOSE AT VARIOUS MFP BY ENERGY GROUPING
F2:P 1 2 3 4 5 6 7 8 9 11 17 23 28 32 36 40
E2 .14999 10 T
FQ2 F U
C
C GAMMA DOSE FUNCTION FROM CALCULATIONS
DE 0.001 0.0015 0.002 0.003 0.004 0.005 0.006
    0.008 0.01 0.015 0.020 0.030 0.040 0.050
    0.060 0.080 0.10 0.15 0.20 0.30 0.40
    0.50 0.60 0.80 1.00 1.50 2.00 3.00
    4.00 5.00 6.00 8.00 10.0 15.0 20.0
C
DF 8.326-10 5.633-10 4.082-10 9.194-10 7.824-10 5.706-10 4.370-10
    2.828-10 1.998-10 2.187-10 2.210-10 1.219-10 7.760-11 5.399-11
    3.988-11 2.456-11 3.166-11 2.538-11 1.881-11 1.180-11 8.779-12
    7.312-12 6.554-12 5.952-12 5.854-12 6.344-12 7.561-12 1.116-11
    1.569-11 2.083-11 2.638-11 3.831-11 5.096-11 8.358-11 1.152-10
C
PRDMP 2J 1
PRINT
NPS 1000000
PHYS:P

```



## VITA

Graduate College  
University of Nevada, Las Vegas

Lawrence P. Ruggieri

### Home Address:

10074 Fort Pike Street  
Las Vegas, Nevada 89178

### Degrees:

Bachelor of Science, Mechanical Engineering, 2006  
University of Nevada, Las Vegas

### Special Honors and Awards:

Most Outstanding Graduate, Mechanical Engineering, Spring 2006  
2<sup>nd</sup> Place Award, Fred and Harriet Cox Senior Design Competition, Spring 2006  
Dean's Honors List

### Publications:

Update to ANSI/ANS-6.4.3-1991 Gamma-ray Buildup Factors for High-Z  
Engineering Materials (Part 1) in Volume 99 of the 2008 Transactions of the  
American Nuclear Society

Thesis Title: Update to ANSI/ANS-6.4.3-1991 for High-Z Materials and Review of  
Particle Transport Theory

### Thesis Examination Committee:

Co-Chairperson, Dr. Charlotta Sanders, Ph.D.  
Co-Chairperson, Dr. Robert Boehm, Ph.D.  
Committee Member, Dr. Brendan O'Toole, Ph.D.  
Graduate Faculty Representative, Dr. John Mercer, Ph.D.